NASA CR-114471
Available to the Public

DESIGN INTEGRATION AND NOISE STUDIES FOR JET STOL AIRCRAFT

FINAL REPORT

Volume I—Program Summary

By J. V. O'Keefe and G. S. Kelley

May 1972

D6-40552-1

Prepared under contract NAS2-6344 by

THE BOEING COMPANY
Commercial Airplane Group
P.O. Box 3707
Seattle, Washington 98124

for
Ames Research Center
NATIONAL AERONAUTICS AND SPACE ADMINISTRATION

DESIGN INTEGRATION AND NOISE STUDIES FOR JET STOL AIRCRAFT

FINAL REPORT

Volume I—Program Summary

By J. V. O'Keefe and G. S. Kelley

May 1972

D6-40552-1

Prepared under contract NAS2-6344 by

THE BOEING COMPANY
Commercial Airplane Group
P.O. Box 3707
Seattle, Washington 98124

for
Ames Research Center

NATIONAL AERONAUTICS AND SPACE ADMINISTRATION

This page is reproduced again at the back of this report by a different reproduction method so as to furnish the best possible detail to the user.

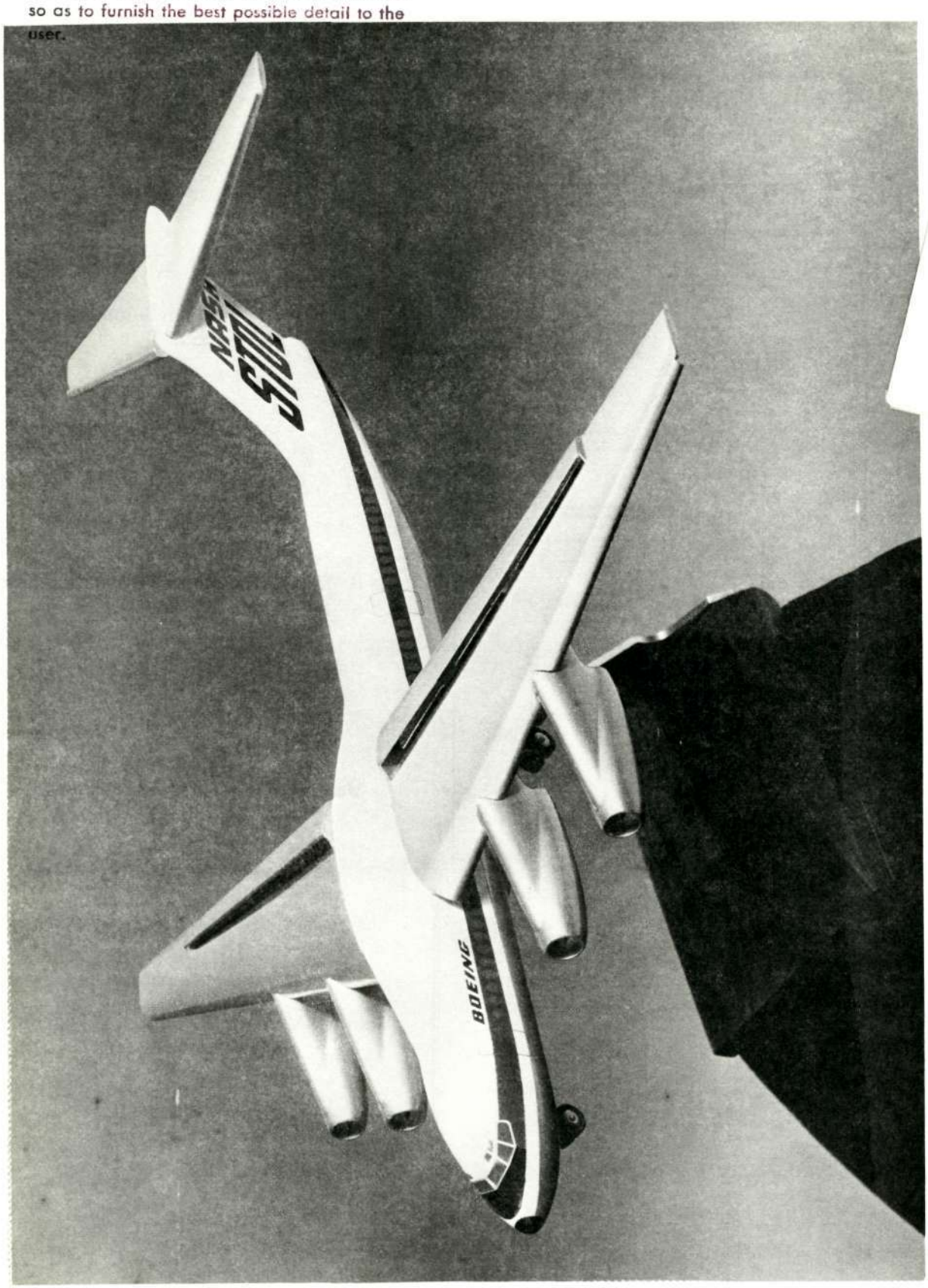

Preceding page blank

DESIGN INTEGRATION AND NOISE STUDIES FOR JET STOL AIRCRAFT

FINAL REPORT

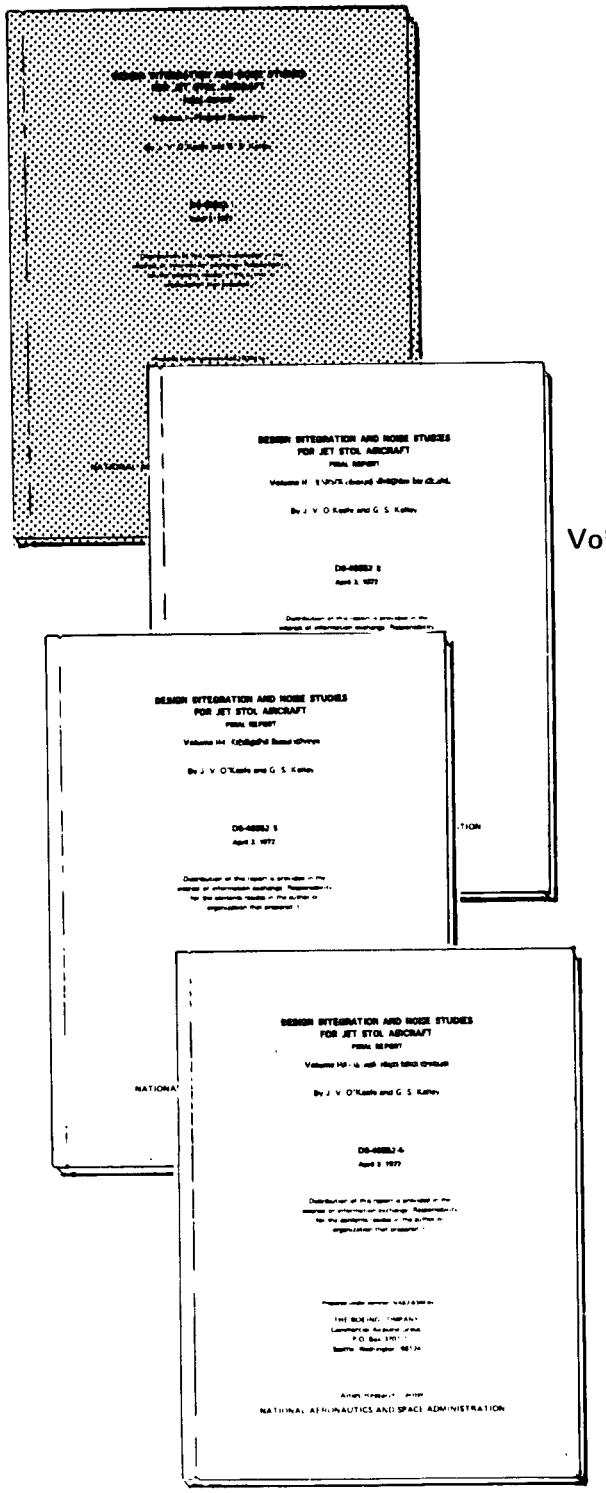

Volume I—Program Summary
D6-40552-1

Volume II—System Design and Evaluation Studies
D6-40552-2

Volume III—Static Test Program
D6-40552-3

Volume IV—Wind Tunnel Test Program
D6-40552-4

CONTENTS

	Page
SUMMARY	1
SYSTEM DESIGN AND EVALUATION STUDIES	4
STATIC TEST PROGRAM	8
WIND TUNNEL TEST PROGRAM	11

DESIGN INTEGRATION AND NOISE STUDIES

FOR JET STOL AIRCRAFT

Volume I—Program Summary

By J. V. O'Keefe and G. S. Kelley
The Boeing Company

SUMMARY

The objective of the Design Integration and Noise Study Program is to develop, through analysis, design, experimental ground rig testing, wind tunnel testing, and design integration studies, an augmentor-wing jet flap configuration for a jet STOL transport aircraft having maximum propulsion and aerodynamic performance with minimum noise. The most significant achievement is the demonstration of 95-PNdB sideline noise at 500 ft, when scaled to a 150-passenger airplane. The schedule and milestones of the program are presented in figure 1.

Static testing in an acoustic arena with a rig of 1/6.4 scale was used for the development of the augmentor noise and thrust characteristics. Basic data were generated for a number of slot and multielement nozzles with various combinations of flaps and flap position.

The good mixing characteristics of multielement nozzles were demonstrated to give a static augmentation ratio of approximately 1.4 with relatively short flaps. Attachment and adequate augmentation were demonstrated at high flap angles for both normal operation and simulated engine-out operation. In total, the augmentor performance development resulted in a practical configuration with characteristics matching the airplane operating requirements.

The development of an augmentor for noise suppression involves the use of multielement nozzles to shift the noise to a higher frequency range amenable to absorption by flap acoustic lining. Suppression was accomplished in a manner very close to precontract predictions. The use of tuned lining was particularly successful. A significant acoustic accomplishment was the development of "screech shields" which interrupt the feedback mechanism causing screech at supercritical nozzle pressure ratios. The effect of these techniques was a suppression of over 20 PNdB at a nozzle pressure ratio of 2.6.

The static rig test program was used to optimize the augmentor configuration on the basis of low noise and high static thrust augmentation. A slot nozzle baseline and two breakup (multielement) nozzles (a round tubular type and a rectangular exit lobe type) were chosen for further development in a two-dimensional wind tunnel test program. These wind tunnel models gave static augmentations in close agreement with those of the larger scale static rig models.

The wind tunnel testing demonstrated that the augmentors with breakup nozzles and those with slot nozzles all had comparable aerodynamic performance. A study of the effect of increasing airspeed showed that the drag polars of an augmentor wing at a constant C_j depend on airspeed while those of an unshrouded jet flap do not.

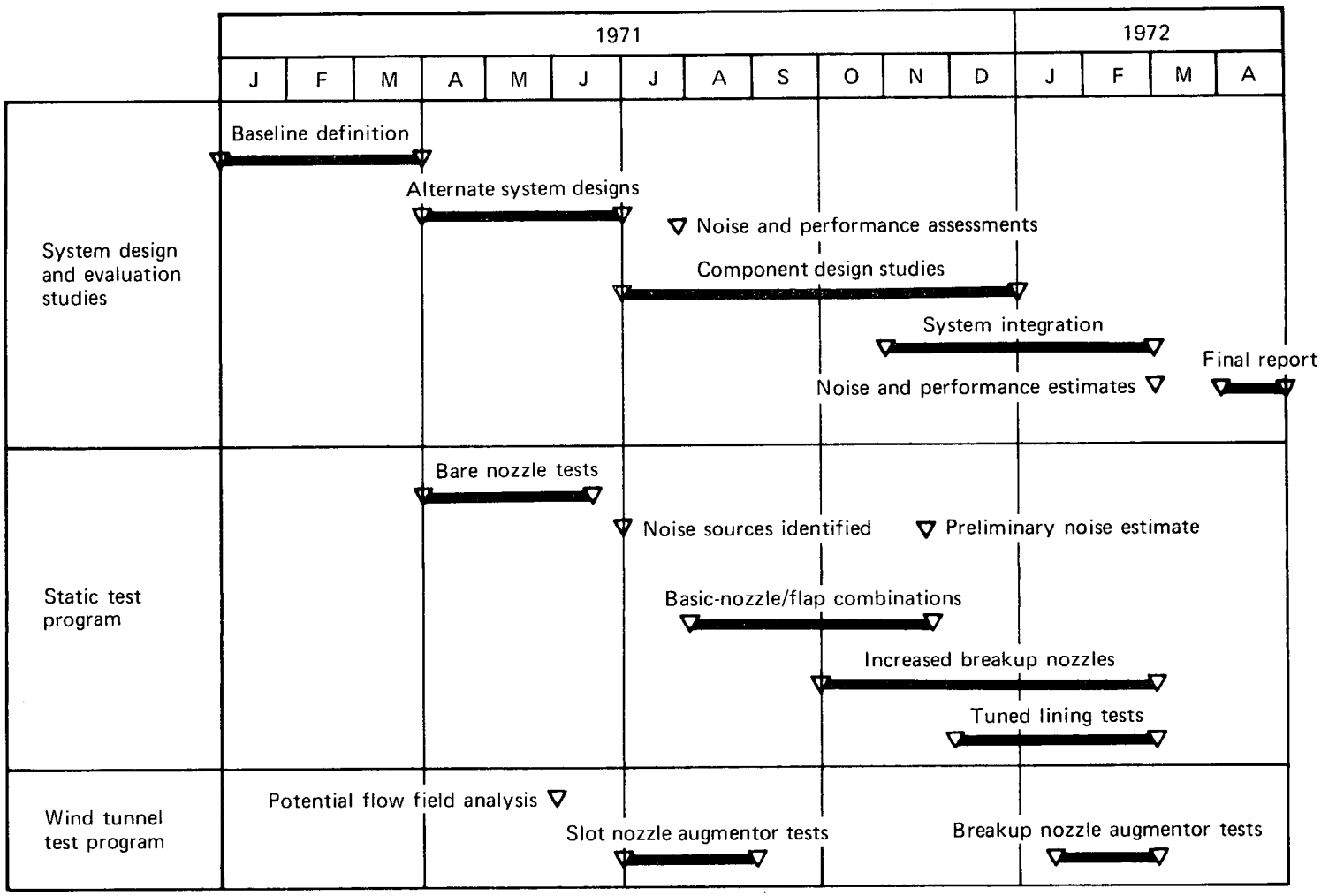

FIGURE 1.–SCHEDULE AND MILESTONES

A system design and evaluation effort was conducted to integrate the test program results in relation to airplane performance. Ducting and augmentor systems were designed in sufficient detail to ensure practical designs and to afford operational tradeoffs in terms of airplane performance. The most significant design parameters considered were engine cycle, wing planform, type of ducting system (independent and plenum), duct pressure losses, engine spanwise location, crossover air for engine-out control, and performance and noise tradeoffs of nozzle and flap geometry.

The two-stream engine concept was developed to show that all of the fan air (80% engine thrust) could be delivered to the augmentor at a nozzle pressure ratio of 2.6, using an independent ducting design for simplified engine operation. The three-stream installation was designed for 40% thrust to the augmentor, resulting in an airplane slightly heavier than the two-stream version and 8 to 10 PNdB noisier.

This contractual effort has culminated in a description of a 150-passenger STOL airplane with 2000-ft field length capability and 95-PNdB 500-ft-sideline noise with characteristics based on technology demonstrated under the contract. This is projected to become a 90-PNdB airplane for 1978 operation with further development work.

A further summation of each program component follows in this volume. Additional detailed data, trade charts, analyses, definitions, and symbols are presented in volumes II, III, and IV as part of this report.

SYSTEM DESIGN AND EVALUATION STUDIES

A system design and evaluation effort was conducted to evaluate test results in relation to airplane performance. The airplane design requirements established were as follows:

Takeoff field length	2000 ft
Range (STOL)	500 nmi
Range (CTOL)	1500 nmi
Cruise	Mach 0.8 at 30,000 ft
Noise target	95 PNdB at 500-ft sideline

Various wing planforms in aspect ratio from 5.0 to 7.5 and sweep angle from 20° to 30° were evaluated to establish the effect of wing geometry on available space for augmentor system installation and the resulting thrust, weight, and airplane performance.

Duct systems, including interconnected engines (plenum) and independent arrangements, were sized and analyzed for a range of internal flow loss and blowing nozzle pressure ratios, with trades against wing rear spar location and engine spanwise location. The independent duct scheme was selected for its inherent advantages in safety, reliability, and simplicity of engine operation.

Engine cycle analyses were performed to provide a consistent basis for applicable parameters including pressure ratio, bypass ratio, weight, size, specific fuel consumption, thrust lapse rate, and primary jet noise. Cycles of proposed engines were established by adjusting the bypass ratio to obtain primary jet velocity and noise compatible with other noise sources. Forward arc (inlet noise) is not a subject of this study; however, a variable-geometry sonic choking device was assumed in the noise and weight analyses. While the main emphasis was on the two-stream engine system with 80% blowing thrust, a three-stream system with 40% blowing thrust was studied for comparison.

Sufficient conceptual design and structure integration of blowing system components was completed to permit weight estimates and to establish realistic allowances for installation space, flexure, thermal growth, and supporting structure.

Using the results of the associated test programs illustrated in figures 2 and 3, the augmentor nozzle and flap configuration were chosen for the minimum airplane takeoff gross weight, TOGW, that would meet the 90-PNdB noise objective.

Airplane characteristics are summarized in figure 4, which gives major parameters as a function of aspect ratio, AR, for a wing sweep angle of 25°. This led to selection of AR = 6.5 with an airplane TOGW of 189 000 lb (STOL). While a small reduction in weight might be realized at slightly higher aspect ratios, the curves reach a limit near AR = 6.8, where maximum installed thrust (T/S duct limit) equals the thrust required for CTOL cruise.

The general arrangement of the airplane is shown in figure 5. Figure 6 summarizes the effects of important parameters studied; the aircraft weight for a range of wing and thrust

loadings is shown, along with limitations incurred by duct volume, cruise, fuel volume, and field length.

The airplane design is summarized as follows:

TOGW (STOL)	189 000 lb
TOGW (CTOL)	230 000 lb
OEW	132 000
Payload	150 passengers
Engines	Four P&WA STF-395D (BM-1) at 18 600 lb SLST
Fuel capacity	70 000 lb (CTOL mission)
W/S (STOL)	87 psf
T/W (STOL)	0.39
Wing:	
Area	2179 sq ft
Aspect ratio	6.5
Sweep angle (0.25c)	25°
t/c	16.4%-12.0%
Tail $\bar{v}$, horizontal	1.07
Tail $\bar{v}$, vertical	0.108

The wing area of 2179 sq ft permits fuel volume adequate for the 67 770-lb requirement of the 1500-nmi CTOL mission.

The projected peak 500-ft sideline noise of the 1978 augmentor wing airplane is 90 PNdB, which is 5 PNdB quieter than the 1972 airplane. The takeoff noise "footprint" generated at maximum STOL takeoff weight is given in figure 7. The 90-PNdB closure point directly under the flight path is located at 7200 ft from brake release. The takeoff noise area encompassed by the 90-PNdB iso-contour is approximately 100 acres measured from the runway end. This type of "footprint" should be acceptable for a great majority of STOLports, especially since the noise spectrum will not contain sharp, pure tones. Although the specific STOLport and community distance relationship is of extreme significance, a 90-PNdB transient-type transportation noise will blend with most community ambient noise levels and result in minor annoyance.

In order to provide maximum wing thickness for the augmentor installation, without penalizing cruise speed, a supercritical wing section was used. Figure 8 shows pictorially the arrangement of the duct and nozzle system, which provides constant spanwise distribution of C_j to the flaps and adequate cross-body flow. The figure includes a section illustrating typical integrated support structure and the relation of the augmentor flap geometry in the approach and stowed modes. The volume requirements for the multielement nozzle array, secondary air ventilation, screech suppressor, and acoustic lining were derived from test results reported in volumes III and IV.

As mentioned previously, the duct-volume-limited installed thrust together with system and structural weight are major factors in the choice of the wing planform. The sensitivity of the mission-sized airplane to significant parameters in the system is given in figures 9 through 15.

The parameter wing thrust loading, T/S, was found to be a useful index in comparing the available duct volume and thrust delivered by the engine. Examination of figure 6 shows that increasing the effective thrust, either by increasing wing thrust loading or by improving the augmentation increment, permits higher wing loading and/or reduction in engine size. The effects of varying wing thrust loading and augmentation increment are compared in figure 9 in terms of the resultant change in OEW of the base airplane. A 10% improvement in augmentation increment or T/S represents 0.3% and 0.6% reduction in OEW, which is equivalent to 1000 and 2000 lb, respectively, in STOL takeoff gross weight. The unfavorable weight trend with decreasing wing loading is also apparent.

The effect on T/S of significant wing geometry variables is given in figure 10. These include aspect ratio, thickness, t/c, engine spanwise location, and rear spar location, all of which directly affect space available for duct and nozzle installation. Wing thrust loading capacity is affected strongly by aspect ratio, and somewhat less by rear spar location.

Critical flow areas in the ducts were found to occur at the engine locations, thereby forcing the nacelles inboard. The locations at 25% and 45% b/2 were selected as the farthest inboard permissible without excessive nacelle-to-body and nacelle-to-nacelle interference drag.

Duct performance in terms of thrust and weight effects is directly related to the flow loss, $\Delta P/P$, of the several components comprising the system, and nozzle pressure ratio, NPR. Both variables affect the flow capacity of the system, and over the range illustrated in figure 11 (NPR 2.4 to 2.8, $\Delta P/P$ 12% to 16%) have equal impact on thrust. It should be noted that NPR = 2.6 was projected as the probable limit of operation due to noise considerations, and the system was sized around this value. Favorable results of screech suppression tests late in the program assign a relatively small penalty (0.5 PNdB) with increase in NPR to 2.8. If this higher NPR were incorporated in the base airplane, it would cause an increase in propulsion and blowing system weight of about 500 lb, largely due to the heavier, higher pressure ratio engine. When the increased T/S is taken into account, the resulting smaller wing and higher wing loading would reduce the net empty weight of the airplane by 1000 lb. A further reduction could be achieved if, in addition, the duct flow velocities were increased to the 16% $\Delta P/P$ value. The latter assumption entails an element of risk, however, both in the estimates of flow loss and in possible deleterious effects on the physical duct construction, and should be experimentally verified.

The independent air distribution system transfers a certain amount of air across the fuselage to reduce asymmetry with an engine failed. With increasing cross-body flow, less thrust can be accommodated in the wing as indicated in figure 12a. This is primarily due to the space constraint near the engine locations. To minimize the airplane weight penalty associated with reduced wing thrust loading, the system was sized for 27% crossflow, the minimum for a balanced design using the roll moment required for normal maneuvering, as shown in figure 12b.

Engine cycles used in the system studies were adjusted by increasing bypass ratio to reduce primary jet velocity and related noise consistent with the noise of the augmentor. Figure 13 shows the installation weight of the engines and blowing system, 33 000 lb, in the base airplane for 90-PNdB, four-engine, 500-ft-sideline noise. Of this amount, 27 000 lb is assigned to the engine installation. An increase in jet noise would reduce the engine and blowing system installed weight by 270 lb per dB.

The weight for the 40% blowing thrust three-stream system in the AR = 7.5 wing is shown on figure 13 for the engine cycle adjusted to 94-PNdB primary jet noise. A reduction of 1000 lb in blowing system weight relative to the two-stream system is indicated, but heavier engine weight results in a net installed weight increase of 5000 lb. This engine weight stems in part from the basic three-stream engine with its larger nacelle diameter and required acoustic treatment for aft fan noise. Another factor contributing to propulsion system weight of the three-stream engine is the higher basic installed thrust loading in terms of thrust/weight ratio, T/W, required at the design point.

Design of the augmentor nozzle has a strong effect on thrust augmentation (nozzle loss and secondary air entrainment) and noise. Both considerations lead toward a multielement nozzle array. Using the static test results, an array area ratio, AAR (height of array/height of equivalent slot nozzle) of 8.0 with at least one array height extension beyond the secondary fairing is necessary for best thrust performance. Acoustic performance dictates a nozzle element width of less than 0.7 in. to bring the noise spectrum within the frequency range of acoustic lining effectiveness.

Various array combinations, ranging from the basic slot to AAR = 8 with maximum breakup, were evaluated in sufficient detail to establish installation weight, performance, and noise. As shown in figure 14a, noise performance improves with increasing nozzle periphery (smaller element width), but weight increases substantially, particularly with the more complex arrays. Nozzles satisfying the 90-PNdB noise target used for a 1978 airplane range from 1800 lb for the simplest to 2700 lb for the most complex.

Static thrust augmentation performance of the same nozzles is presented in figure 14b, which shows that nozzles with the most breakup and largest array area ratio perform best, but are heaviest. However, when evaluated in terms of the weight to be saved with improved augmentation (115 lb OEW for $\Delta\phi = 0.01$) the simplest, lightest weight nozzle meeting the noise requirement shows a net advantage of 400 lb.

A similar comparison may be made considering the length of nozzle extension versus length of flaps, figure 15. In this case augmentation improves and weight increases with nozzle length. A small advantage in OEW is indicated up to the design point. Beyond that point, further extension of the nozzle results in a break-even between the weight benefits from augmentation and the weight penalty of the nozzles.

A comparison of the two-stream propulsion system weight (including engines, ducting, and nozzles) with that of the three-stream system having 40% blowing thrust showed the three-stream system to be 5000 lb heavier. Since the three-stream total thrust is less restricted by the wing ducts than the two-stream, it was possible to increase the wing aspect ratio to 7.5 compared with 6.5, and the wing loading, W/S, to 95.6 psf compared with 86.75 to gain airframe weight benefits. The TOGW of the three-stream mission-sized airplane is thus only 3100 lb greater than that of the two-stream. However, in evaluating the effects of inlet splitters on the fan rear-arc noise with flap impingement, the resulting 500-ft sideline noise is 99 PNdB compared with 90 PNdB for the two-stream airplane.

STATIC TEST PROGRAM

Static testing during task I included slot nozzles with aspect ratios between 50 and 400, a convergent-divergent nozzle, and various multielement nozzles with lobe and tube shapes. The results are presented in section 6.0 of the task I report. Subsequent static testing included augmentor flap systems with task I nozzles and improved nozzles. The results presented in this report show how the noise and performance objectives are met with the augmentor.

The static testing included multirow tube and lobe nozzles of array area ratios varying from 4 to 8. Several configurations of augmentor geometries with internal design variations were investigated with a variety of acoustically tuned linings. Combinations of flap and shroud lengths were tested for their thrust augmentation and noise characteristics. The best configurations for performance and noise used high array area ratio multielement nozzles in augmentors with symmetrical internal contours, nozzle screech control devices, and tuned acoustic lining. The noise suppression available from one of the best configurations is illustrated in figure 16. The noise objective of 95 PNdB at 500-ft sideline is met by this configuration and the static thrust augmentation level (total thrust vector, flaps on/flaps off) is above 1.42 at takeoff flap setting. The achievement of the large noise suppression required to meet the 95-PNdB noise level depends on a series of carefully integrated design steps. These are shown, starting with a high-aspect-ratio unaugmented slot nozzle and progressing through an augmentor with acoustically tuned lining.

A peak level of 116 PNdB would be measured on the 500-ft sideline at takeoff of a jet STOL aircraft employing a high-aspect-ratio slot nozzle for bypass thrust. A suppression of 21 PNdB, relative to such a slot nozzle, is required to achieve the goal of this task. This suppression is equivalent to a reduction of annoyance by a factor of 4 to 5. The "noy weighted" spectrum (fig. 16.) of the slot nozzle identifies the problem area as the mid- and high-frequency range of the spectrum. The annoyance levels in the 2- to 4-kHz bands (to which the ear is most sensitive) are particularly prominent. While a large array area ratio (AAR) multirow lobe nozzle alone alleviates the midfrequency band level problem (fig. 16), the effect in the critical high-frequency bands is only enough to deliver a suppression of 6 PNdB.

Adding an unlined augmentor to the lobe nozzle reduces the noise level in high-frequency bands, but increases noise in the low-frequency bands; the result is a noise suppression of 4 PNdB for a net of 10 PNdB. Additional reductions of noise in higher frequency bands are achieved by installing acoustically tuned lining in the augmentor flap, by screech suppression, and by baffling. By adding tuned lining to the internal augmentor surfaces, the noise is suppressed by 3.5 dB. When screech shields are added, the combination of screech elimination and improved operation of the tuned lining suppresses the noise by 7 PNdB rather than 3.5 PNdB. (The aerodynamically induced jet screech produced by the multirow lobe nozzle is eliminated by extending one side of each lobe six lobe widths, as illustrated in figure 16.) Finally, by matching the core depths of the tuned lining to the frequency distribution along the jet axes and installing a baffle at the lower secondary air gap, the noise was suppressed by another 2 PNdB to achieve a total suppression of 21 PNdB, the goal of the task.

High static thrust augmentation is developed with multirow lobe nozzles of large array height operating with a relatively short augmentor system. The multielement nozzles in augmentors demonstrate high static thrust augmentation through 45°of internal flow turning without the need for special boundary layer control slots on the flap or other devices for energizing the boundary layer (fig. 17).

The relationship between the achievable augmentation ratios, nozzle array area ratios, and nozzle ventilation is illustrated in figure 18. As the nozzles increase in length, in array area ratio, in number of elements, and in nozzle perimeter, the augmentation ratio increases from 1.2 to 1.48 (figs. 17 and 18).

Since thrust augmentation does not include nozzle internal loss effects, these must be identified to evaluate airplane performance. The velocity coefficients of the suppressor nozzles tested correlate well as a function of hydraulic diameter (fig. 19); the penalties associated with nozzles having large numbers of elements are predictable. The velocity coefficients from the curves of figure 19 are the maximum to be expected.

Static test results with the multielement nozzle/augmentor indicate adequate airplane performance with an engine out. Final determination, however, must be made in wind tunnel tests. The augmentor flow characteristics should permit the augmentor flap to provide good wing aerodynamic lift coefficients and successful lateral control. A nozzle arrangement providing high static thrust augmentation during engine-out operation is shown in figure 20. With either one- or two-thirds of the augmentor primary nozzles operating, performance levels are equal to or above the all-engines-operating conditions.

Compromises must be made in order to satisfy airplane requirements. One of the most important factors in augmentor wing airplane designs is the trade-off in augmentor system length. Although increasing the nozzle length significantly improves augmentation (fig. 18), no change in noise suppression was measured. Increasing the flap length, however, provides both acoustic and augmentation improvement (fig. 21). Within the range of lengths considered, it is important to use as long an augmentor as possible.

Significant augmentation advantages are available from augmentor configurations with high-AAR primary nozzle systems (figs. 17 and 18). There is only a small acoustic penalty for increasing the array area ratio of the primary nozzles (fig. 22). This penalty does not change when the lining is added to the inner augmentor surfaces.

An important element in obtaining the 21-PNdB noise suppression is the proper design and application of tuned lining for the augmentor surfaces. This was accomplished by testing a matrix of seven linings. The best lining was in the "eye" of the matrix, confirming the design procedure. This lining achieved 3-1/2-PNdB suppression relative to the unlined augmentor. The SPL spectrum for this is shown in figure 23.

Although the lining design procedures are successful in selecting the best lining, the initial suppression was below the 6 PNdB predicted. The effectiveness of the acoustic lining was being masked by nozzle screech; consequently, an investigation was made to develop an effective screech suppressor for the primary nozzles. A screech shield was devised and applied to the AAR = 6, 172-lobe primary nozzle, and the tuned lining reduced the noise by 7 PNdB relative to the unlined augmentor. The SPL spectrum for this is shown in figure 24, which

shows a comparison of the lined and unlined augmentor with a slot nozzle at model scale. Of the 7-PNdB reduction, 1 PNdB is due to using two different linings in the axial direction, resulting in a 6-PNdB lining reduction, as predicted.

The spectrum and beam patterns of the best lined augmentor tested are shown in figure 25. The primary nozzle has screech shields; the augmentor has mixed single-layer lining and a lower gap baffle. The SPL spectrum is based on the same data as the "noy-weighted" spectrum in figure 16, and it is compared with a slot nozzle. The suppressed spectrum is flat with no pure tones and varies less than 10 PNdB through the frequency range. The maximum perceived noise level is reduced by 21 PNdB relative to the slot nozzle. The beam pattern of the suppressor is highly directional, providing additional advantages with respect to the time duration effects.

All performance and acoustic tests were performed at the Boeing North Field Mechanical Laboratories in Seattle, Washington. The laboratories have a facility designed for large-scale combined acoustic and thrust performance test programs. The augmentor thrust is measured with a six-component, platform-type balance bridged with high-pressure air; the noise can be measured in a 180° arc in an acoustic arena, as shown in figure 26. The thrust stand accurately measures model forces using either hot (300° F) or ambient-temperature air. Nozzle flow rates are determined with precision using ASME venturi flow meters calibrated against a Boeing standard nozzle. An acoustically treated muffler plenum, located on the balance platform upstream of the test nozzle plenum, prevents noise generated by the air supply lines and control valves from reaching the test nozzles. A flap system is shown installed on the test stand in figure 27.

To ensure data repeatability, a round convergent reference nozzle was tested periodically throughout the test program. During each check the nozzle velocity and discharge coefficients were compared to previous levels to detect instrumentation malfunctions and check the force balance calibration and repeatability. The force balance was also independently calibrated periodically throughout the test program using a hydraulic loading device in series with a standard load cell.

The long-term repeatability of the nozzle performance is shown in figure 28. The combined repeatability of the thrust and airflow data are within ±0.7%. Airfow repeatability is 0.4%; thrust repeatability is ±0.5%. The acoustic data repeatability was maintained such that the standard deviation, 1σ (fig. 29) is less than ±0.4 PNdB when data are scaled and extrapolated to a 500-ft off-axis distance. The probable error in level for all acoustic measurements lies between 1.5 and 2.5 PNdB over the measured frequency range.

A review of the major acoustic milestones is given in figure 30. The estimated curves were presented in reference 2. Measured noise levels are shown for one nozzle pressure ratio, 2.6. Good agreement is obtained with predicted values, and the goal of 95 PNdB is achieved. The objective of future tasks is to improve the noise suppression by 5 PNdB and the thrust augmentation ratio by five counts (a "count" is 0.01 in $\Delta\phi$). The acoustic improvment lies primarily in the area of the application of multielement acoustic linings, while the thrust improvement lies in the area of better mixing primary nozzles, improved nozzle ventilation, and refinements in internal augmentor contours.

WIND TUNNEL TEST PROGRAM

The aerodynamic characteristics of four augmentor wing configurations were evaluated by two-dimensional wind tunnel tests in the 3- by 8-ft Boeing low-speed research tunnel. The purpose is to develop an augmentor wing configuration having a low noise level and good aerodynamic performance during takeoff and landing. Configurations with multielement nozzles, having lower noise and better propulsive characteristics than slot nozzle augmentors, have been developed on the static test rig (see vol. III). These configurations were further developed in the wind tunnel and their performance compared with that of the slot nozzle augmentor flap derived from NASA/DHC design.

The wind tunnel study showed that the multilobe nozzle augmentor flap configuration possesses aerodynamic characteristics comparable to those of the slot nozzle augmentor. Tests at various airspeeds showed that the thrust augmentation properties of an augmentor wing are partially offset by ram drag. In contrast to a plain jet flap, the force coefficients of an augmentor flap cannot be correlated by the nozzle thrust coefficient alone.

The NASA scaled model, having a 16-in. chord and 3-ft span, was tested over ranges of airspeed varying from 0 to 115 kn, primary nozzle to ambient pressure ratio varying from 1.0 to 3.8, and flap deflection varying from 30° to 70°. The results presented are based on the three-component balance measurements, model surface pressures and augmentor exit total pressure data, and measurements related to blowing and air stream parameters.

CONFIGURATIONS

The principal features of the four augmentor wing configurations are listed below.

Configuration	Type of Primary Nozzle	Flap Chord/ Wing Chord	Flap Exit Area/ Nozzle Exit Area
NASA wing section	Continuous slot	0.35	100
Scaled NASA section	Continuous slot	0.27	50
Lobe nozzle augmentor	Multilobe	0.27	57
Tube nozzle augmentor	Multitube	0.27	50

The two augmentors with slot nozzles are shown in figure 31. The NASA wing section represents a streamwise section of the NASA Ames swept-wing STOL model (NASA TMX-62029). As a result of sizing studies presented in volume II, the NASA augmentor flap segments were scaled down to give a 0.27 flap chord and the slot height increased to provide the desired thrust per wing area.

The two augmentors with different multielement nozzles used the same flap segments. The geometry of the lobe and tube nozzles is shown in figure 32 and that of the flap segments in figure 33. The internal contours of the augmentor flap assembly were developed from static rig tests described in volume III. The external contours were designed using a semiempirical method developed in task I.

Leading edge geometry is illustrated in figure 31. The 0.15 c leading edge slat was used only on the NASA wing section. The other three configurations incorporated the 0.11 c leading edge flap designed at Boeing for use with leading edge blowing boundary layer control.

For each augmentor configuration, geometry variations to improve the aerodynamic performance were carried out by repositioning model parts at every flap angle. The extent of this process varied from one configuration to another. The effects of the following changes were studied to evaluate configuration sensitivity:

- Flap chord and augmentor mixing length
- Shroud position
- Intake door angle
- Flap coanda position
- Diffuser angle
- Throat area
- Lobe nozzle sealing to reduce ventilation (see fig. 33)
- Wing leading edge geometry
- Wing leading edge boundary layer control (BLC)

TEST PROGRAM

The wind tunnel tests were accomplished in three separate periods:

Test Period	Test Objective
June 1 to July 20, 1971	To evaluate the aerodynamic characteristics of the two slot nozzle augmentors
January 18 to January 28, 1972	To evaluate the effects of airspeed on the aerodynamic performance of the slot nozzle augmentor at 30° flap angle
February 5 to March 3, 1972	To evaluate the aerodynamic characteristics of the two multielement nozzle augmentors

The test procedure was to carry out geometry optimization and then select the best configuration on the basis of static and q = 20 psf force data at a nominal design thrust level (nozzle pressure ratio (NPR) of 2.5 to 2.8). For this configuration, a complete series of constant nozzle pressure ratio and varying angle-of-attack runs was then made. This procedure was repeated for all flap angles tested, except in the case of the NASA wing section.

TEST RESULTS

Aerodynamic Characteristics

The aerodynamic performance of an augmentor wing depends strongly upon avoiding flow separation from the shroud upper surface. Shroud flow separation tends to increase with flap deflection, angle of attack, and reduction of nozzle thrust coefficient. It has also been

found to depend upon intake door angle and shroud and flap position. In general, at $\delta_f = 30°$ and 50° complete flow attachment was achieved at the C_j's of interest, but this was not the case at $\delta_f = 70°$. The best data obtained for $\delta_f = 70°$ were with a low shroud position, as shown in figure 33. Representative force and pitching moment data at a thrust coefficient, C_j, of 1.16 are shown in figure 34 for the scaled NASA section and optimum geometry at each flap deflection. The variation of force data with C_j is summarized in figure 35. The shapes of the C_l vs C_j curves indicate that the C_j required for flow attachment is considerably higher than in the case of a plain jet flap (sometimes known as a blown flap or jet augmented flap). The thrust effectiveness* represented by the variation of C_X with C_j at a constant C_l are about 1.2 for $\delta_f = 30°$ and 50°. The data points at $C_j = 1.8$ in figure 35 correspond to an NPR = 3.5. At that condition, performance was degraded noticeably by the change in flaps-off jet path, which would require a change in flap (coanda) position.

The sensitivity of performance to the flap position relative to the jet path was extensively demonstrated by the results presented in volumes III and IV of this report. The failure to achieve a reasonable performance level with the NASA wing section, particularly at high flap angles, is attributed to the nonoptimum flap position. The results for the two slot nozzles augmentors are compared in figure 36, which clearly illustrates the performance degradation of the NASA wing section at $\delta_f > 40°$. This configuration was repositioned at $\delta_f = 50°$, and substantial improvements are shown.

For every configuration tested at forward speed, the static reaction was also measured to determine the static thrust augmentation ratio. The significance of this quantity is illustrated by its relationship to aerodynamic performance. In general, increases in static thrust augmentation are manifested in streamwise force data at low flap angles. This is evident in figure 37, where variations of C_X at constant C_l with ϕ are shown for $\delta_f = 30°$ and 50°. The variation of ϕ for the configurations having the same δ_f is generally due to small differences in throat area, diffuser angle, or flap position. The drag polars, not shown in the figure, are well behaved and do not cross except near stall. The change in streamwise force coefficient at a constant C_l represents a shift in the drag polar. Similar relationships between C_X and ϕ cannot be established at $\delta_f = 70°$.

The above findings from slot nozzle augmentor tests are equally valid for multielement nozzle augmentors. The aerodynamic performance of the lobe nozzle augmentor was compared with that of the tube nozzle augmentor at $\delta_f = 50°$ only. The differences are generally small. Since the lobe nozzle augmentor had significantly lower noise level than the tube nozzle augmentor (see vol. III), the former was extensively developed in the wind tunnel test.

The variation of force coefficients with C_j is shown in figure 38 for the lobe nozzle augmentor. The trends are similar to those shown in figure 35 for the slot nozzle augmentor. A significant improvement was found at $\delta_f = 70°$ when the nozzle ventilation from the lower side was reduced by sealing tape (see fig. 33). Tufts observation indicated that taping improved the flow over the nozzle boattail and the intake door at $\delta_f = 70°$. Taping was not tried at $\delta_f = 50°$, but at $\delta_f = 30°$ it resulted in a small lift increment accompanied by a thrust decrement. The effects of taping are also illustrated in figure 38.

*Thrust effectiveness is defined as the rate of change in streamwise force with primary nozzle thrust, i.e., $\partial C_X / \partial C_j$.

The aerodynamic performance of the lobe nozzle augmentor compared quite favorably with that of the slot nozzle augmentor at $\delta_f = 30°$ and 70° but was inferior at $\delta_f = 50°$. However, the difference at $\delta_f = 50°$ is expected to become insignificant if nozzle ventilation is restricted. Since nozzle ventilation effects have only been briefly explored, further study is highly recommended in view of their demonstrated effect on aerodynamic performance and potential effect on noise properties.

The effect of leading edge blowing BLC on the aerodynamic performance of an augmentor wing was investigated. The primary effect was to delay stalling and increase maximum lift, as expected. The rate of recovery of the blowing momentum as thrust was generally less than 0.6. Compared to a thrust effectiveness, $\partial C_X / \partial C_j$, of 1.2 for the augmentor primary thrust, leading edge blowing is not an efficient means for thrust augmentation.

Effect of Airspeed Variation

The approach taken to evaluate the thrust augmentation characteristics of an augmentor wing as a function of forward speed is to use the forward speed characteristics of a plain jet flap as the base. The plain jet flap is chosen because its characteristics are well understood and considerable experience has accumulated in applying wind tunnel data to predict airplane performance. The difference in the forward speed effects for the two configurations forms the basis for modifying the established method used for jet flap airplanes so that it applies to augmentor wing airplanes.

The data addressed to the airspeed effects were taken primarily on typical takeoff configurations, $\delta_f = 30°$, for two reasons: (1) the effect of airspeed on the streamwise force is particularly important during takeoff and (2) the shroud upper surface is relatively free of flow separation.

The configurations included two scaled NASA slot nozzle augmentors with different throat areas, one lobe nozzle augmentor, and one jet flap with slot nozzle. All three configurations have a 0.27 c flap chord.

The results showed that the drag polars at a given C_j are essentially independent of airspeed for the jet flap but not for the augmentor flaps. Typically, the variations of C_X with airspeed at $C_j = 0.8$ and $C_l = 4$ are illustrated in figure 39 for the jet flap and the three augmentor flap configurations. While C_X is essentially constant for the jet flap, it varied substantially with airspeed for the augmentors. However, the C_X for the augmentors is more negative (more thrust) than that of the plain jet flap. For each augmentor, a minimum drag occurred at some airspeed between 60 and 80 kn. The variation of C_X, though not the level, is reasonably well approximated by the sum of ram drag and augmented thrust, $2C_q - \phi C_j$, shown in the same figure. The differences between C_X and $2C_q - \phi C_j$ are reasonably (within ±0.01) independent of airspeed, which allows one to predict the performance at various airspeeds based on data taken at static and one forward speed condition.

The fact that static thrust augmentation and entrainment can be used to correlate forward speed data suggests that the ejector internal flow is little affected by airspeed. Both static pressure distribution and augmentor exit total pressure data support this hypothesis.

At a given primary nozzle thrust, the drag increase with forward speed at either constant or constant C_1 was more rapid with the augmentor than with the jet flap. The source of the additional drag experienced by the augmentor has been identified through an analysis of static pressure distribution. Pressure drag of the intake and the shroud, which includes a large part of ram drag, was the major contributor.

The Boeing Company
P.O. Box 3707
Seattle, Washington 98124, May 22, 1972

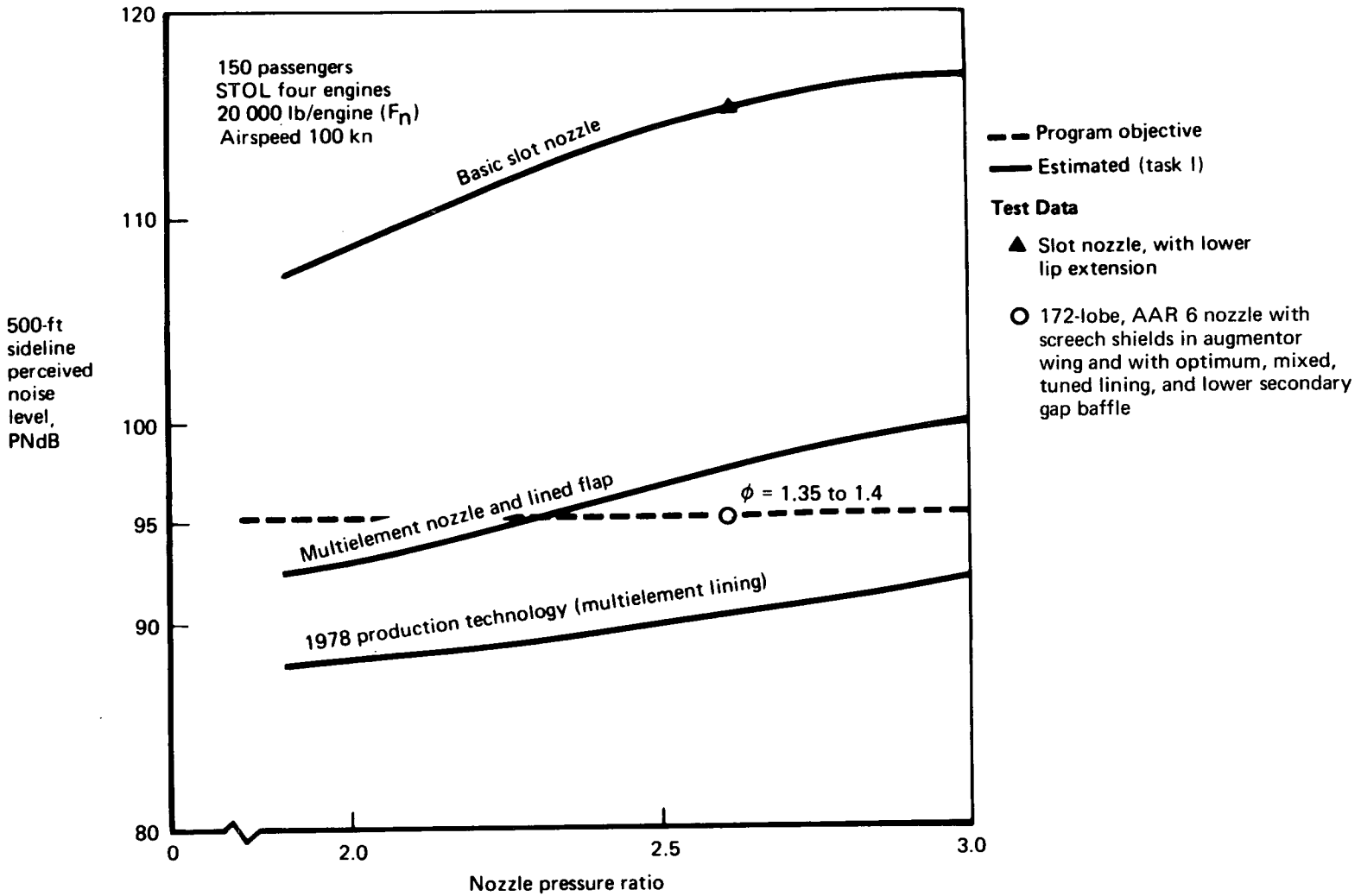

FIGURE 2.– AUGMENTOR WING NOISE LEVELS

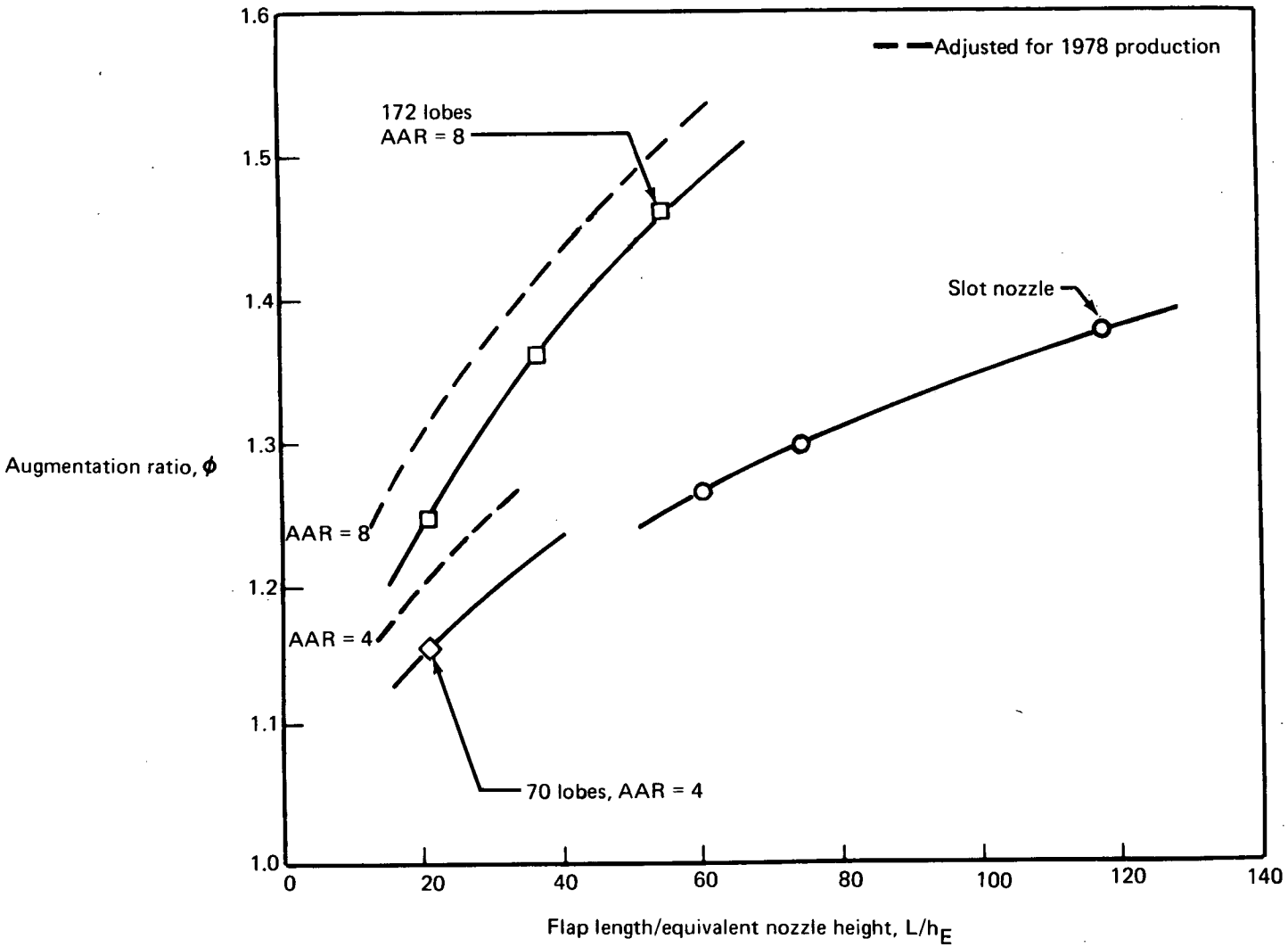

FIGURE 3.–AUGMENTOR TEST PERFORMANCE

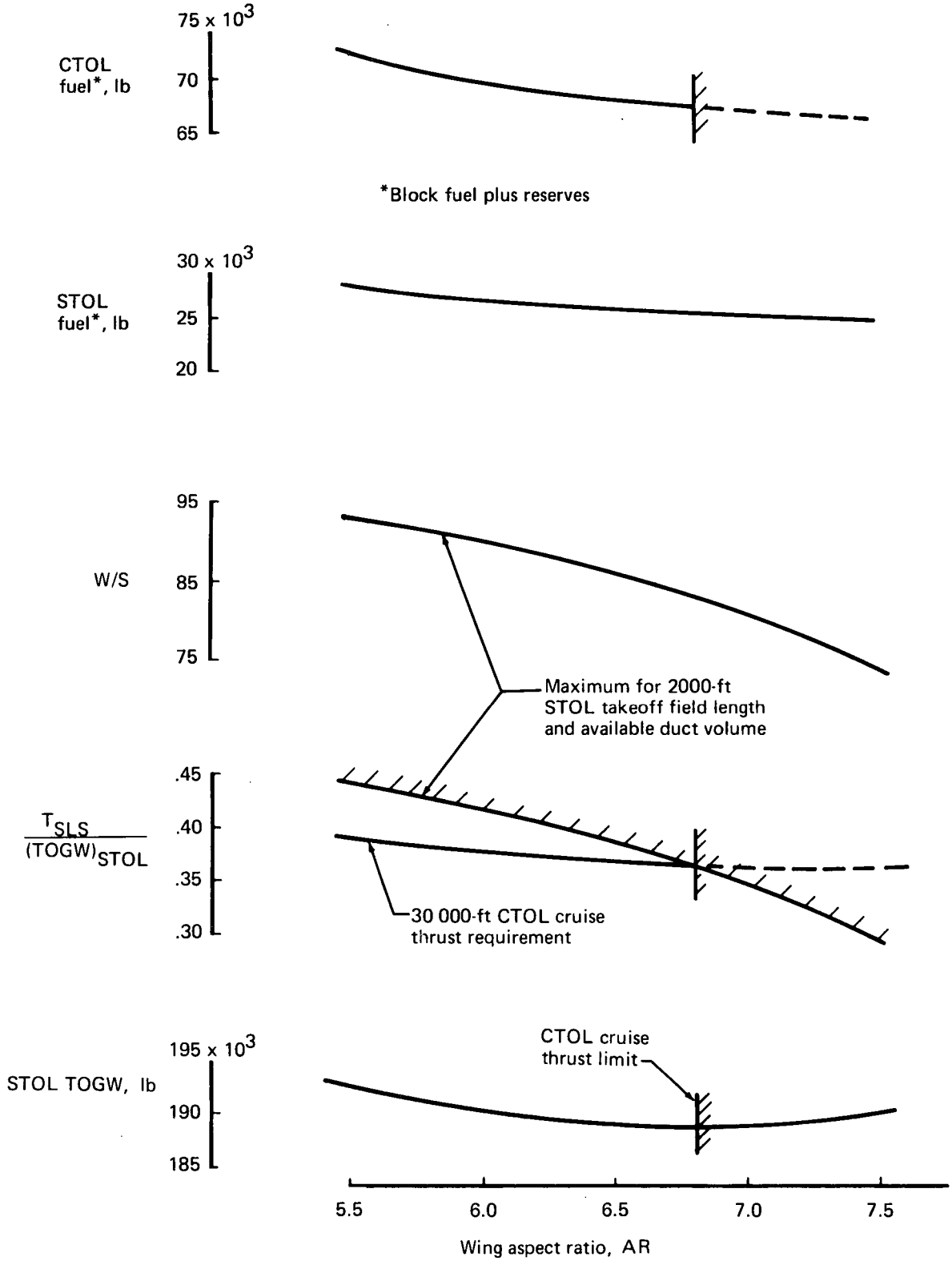

FIGURE 4.—SUMMARY OF PLANFORM EFFECTS ON AIRPLANE CHARACTERISTICS

TOGW (STOL)	189 000 lb
TOGW (CTOL)	230 000 lb
OEW	132 000 lb
Fuel capacity	70 000 lb
Payload	150 passengers
Engines	Four P&WA STF-395D (BM-1) at 18 600 lb SLST
W/S (STOL)	87 psf
T/W (STOL)	0.39
Wing	
Area	2179 sq ft
Sweep (0.25c)	25°
Aspect ratio	6.5
t/c	16.4%-12.0%
Tail $\bar{v}$, horizontal	1.07
Tail $\bar{v}$, vertical	0.108

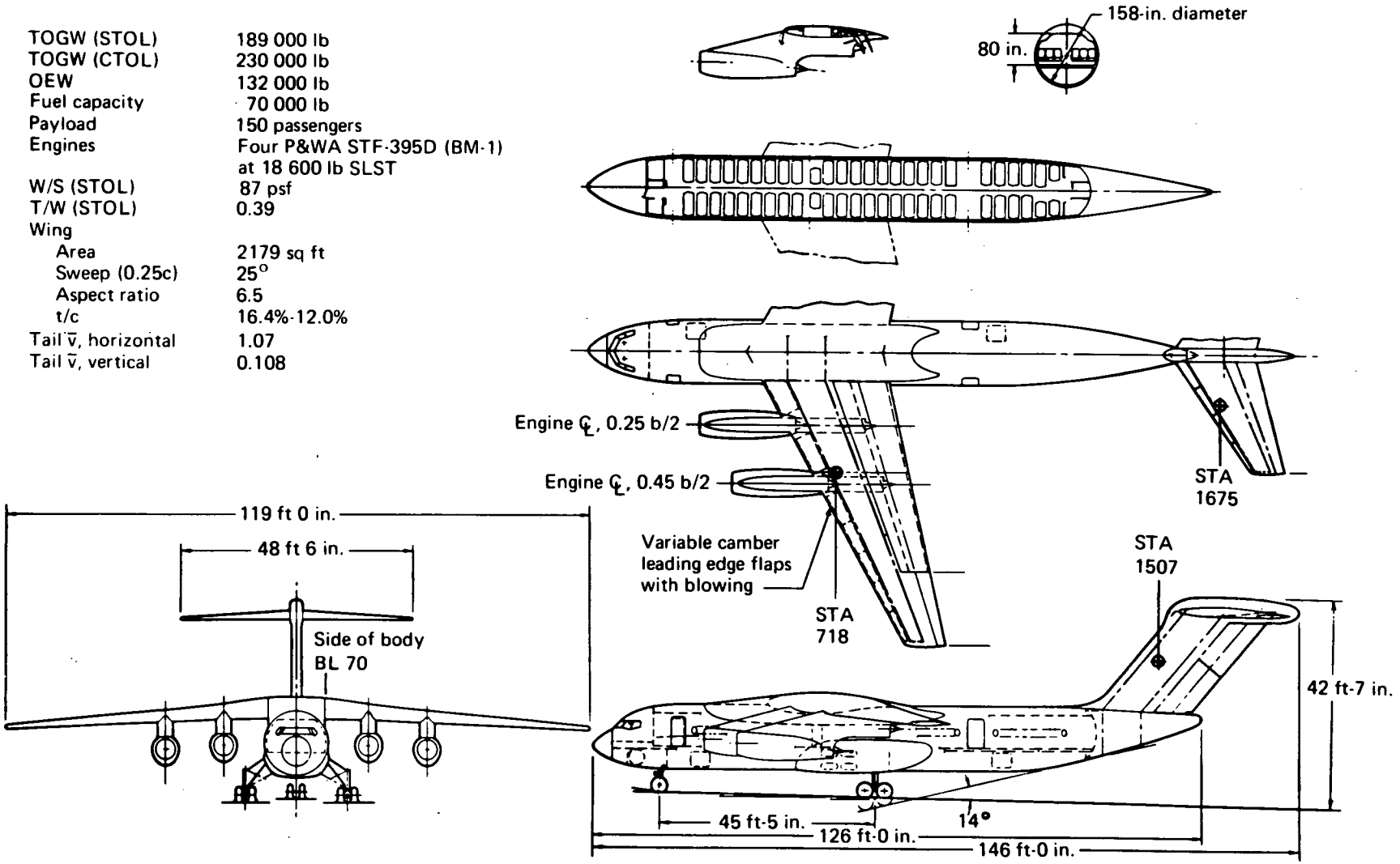

FIGURE 5.–GENERAL ARRANGEMENT, TWO-STREAM AUGMENTOR WING AIRPLANE (MODEL 753)

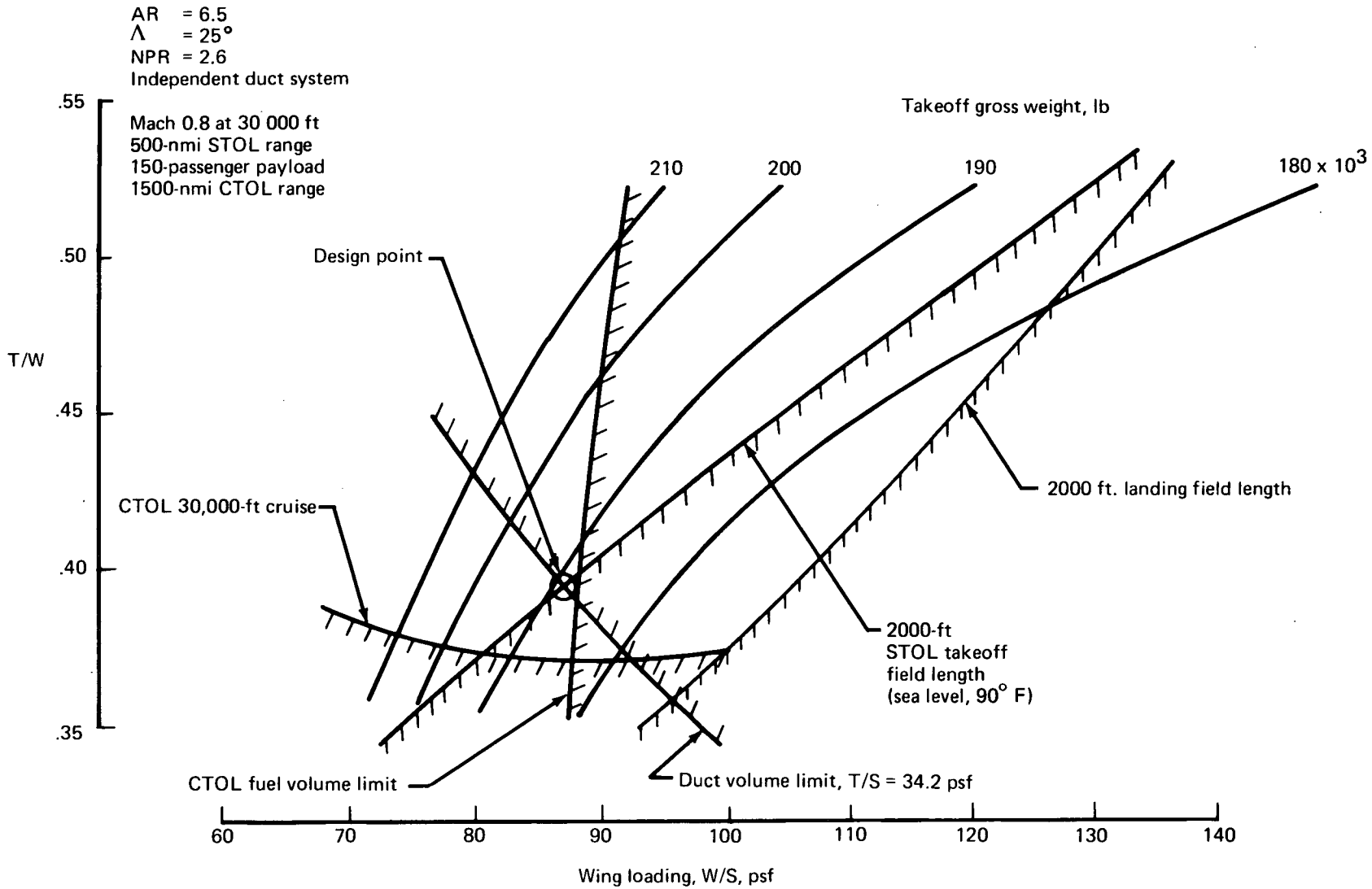

FIGURE 6.—TWO-STREAM AUGMENTOR WING AIRPLANE SIZING PARAMETERS

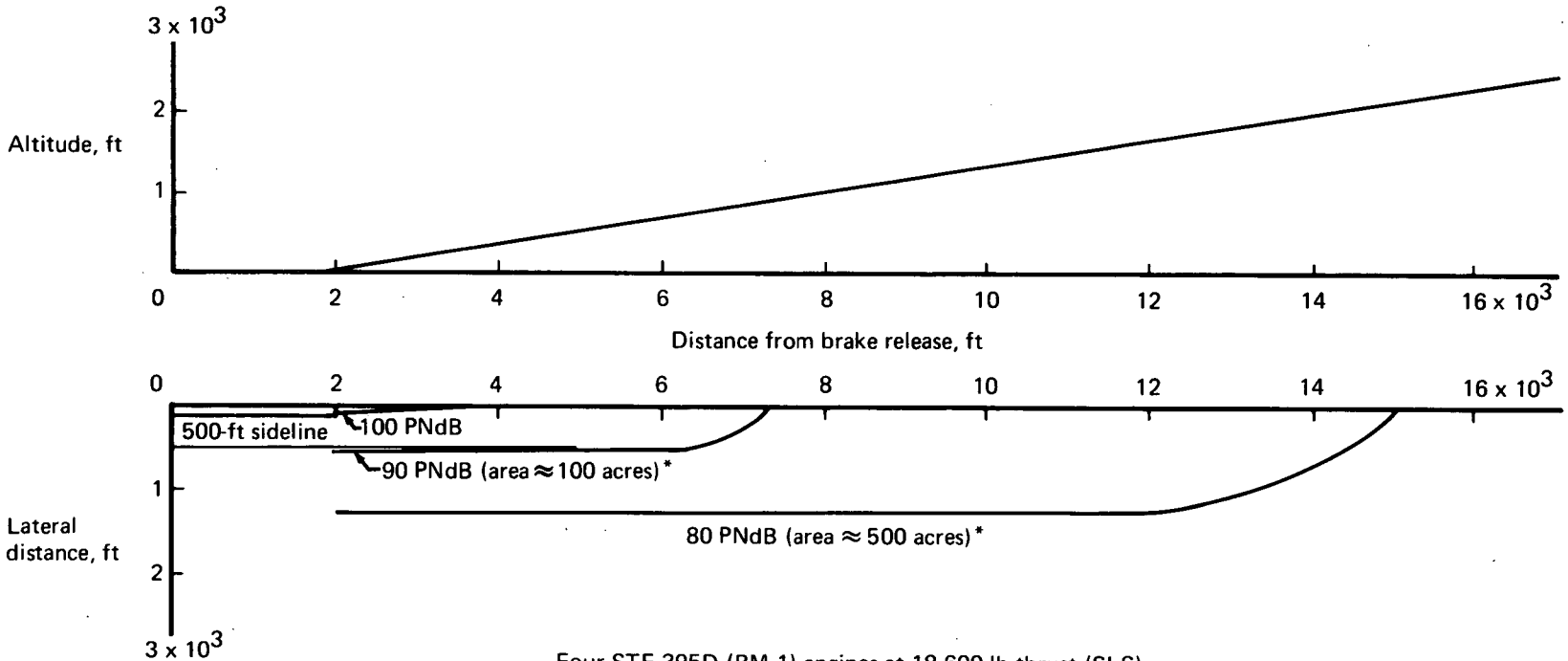

Four STF 395D (BM-1) engines at 18 600 lb thrust (SLS)
Average gradient 0.149
Average airspeed 91 KTAS

*Area measured from end of runway

FIGURE 7.–TAKEOFF FOOTPRINTS FOR TWO-STREAM AUGMENTOR WING AIRPLANE

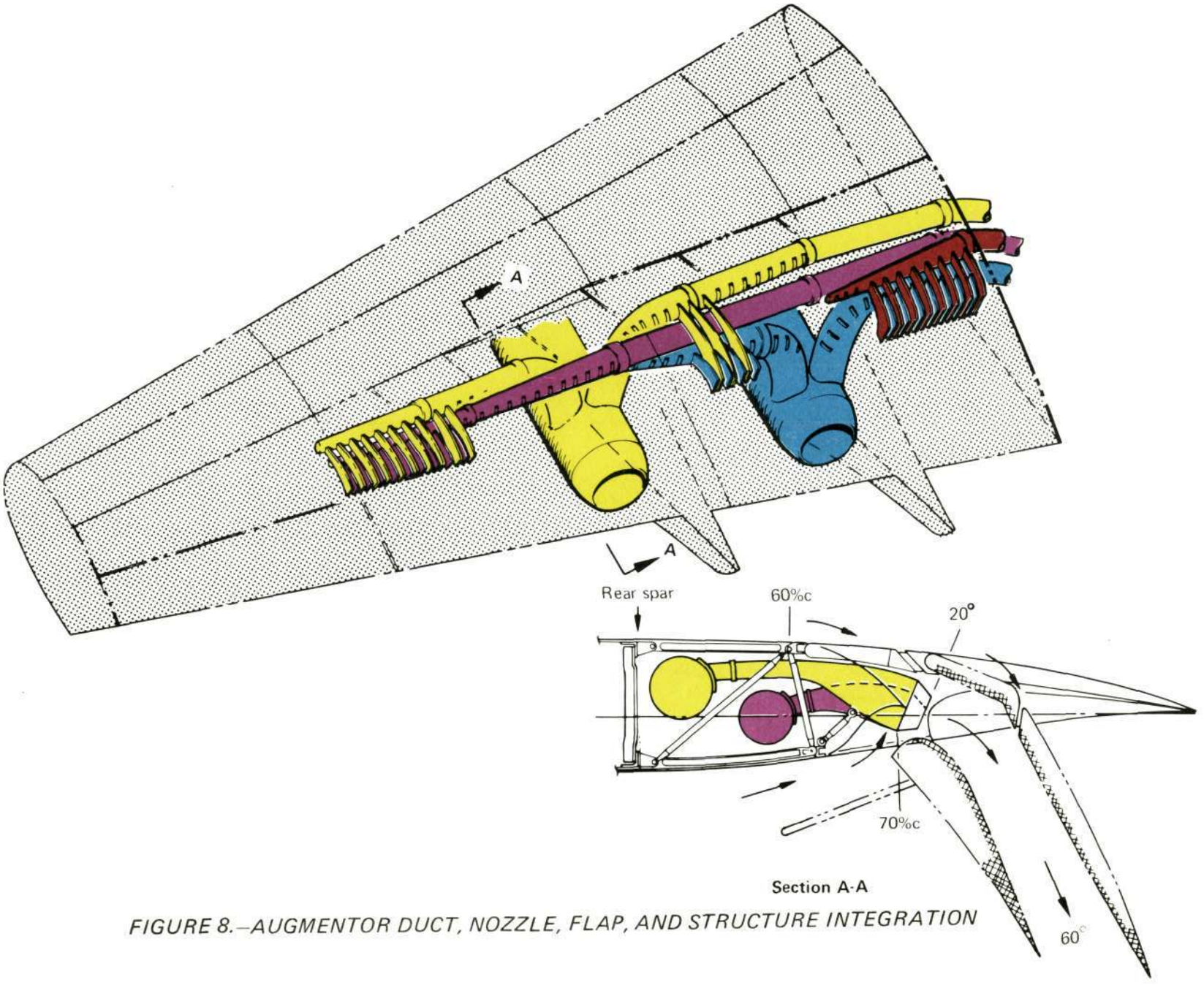

FIGURE 8.–AUGMENTOR DUCT, NOZZLE, FLAP, AND STRUCTURE INTEGRATION

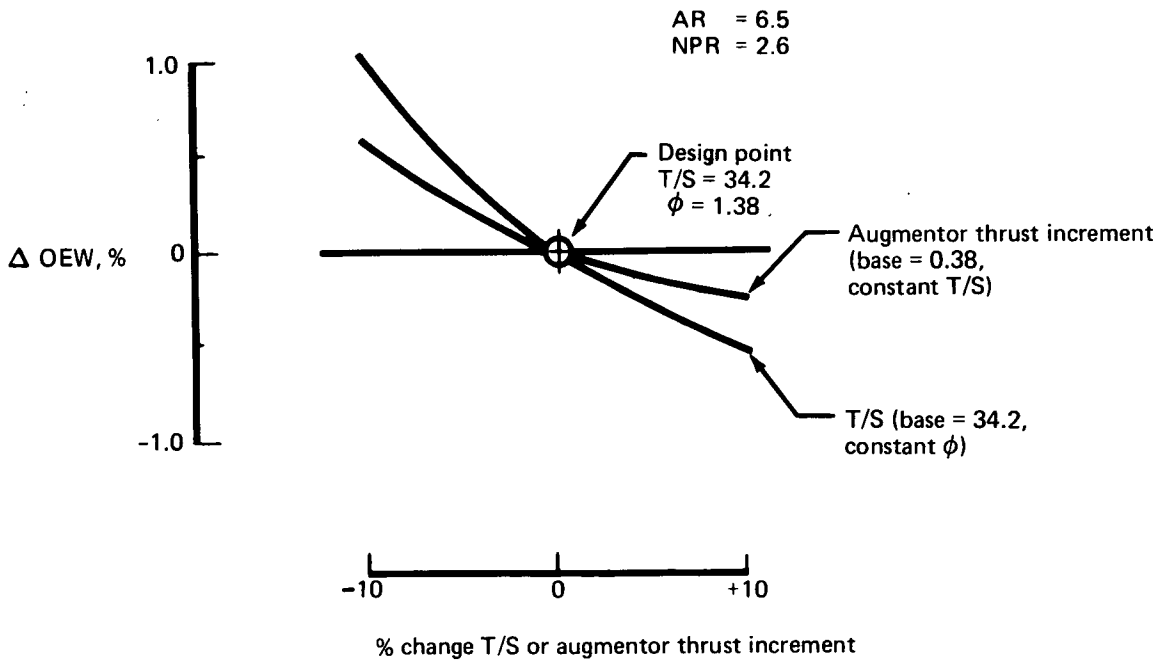

FIGURE 9.—WEIGHT SENSITIVITY TO WING THRUST LOADING (T/S) AND AUGMENTOR THRUST INCREMENT

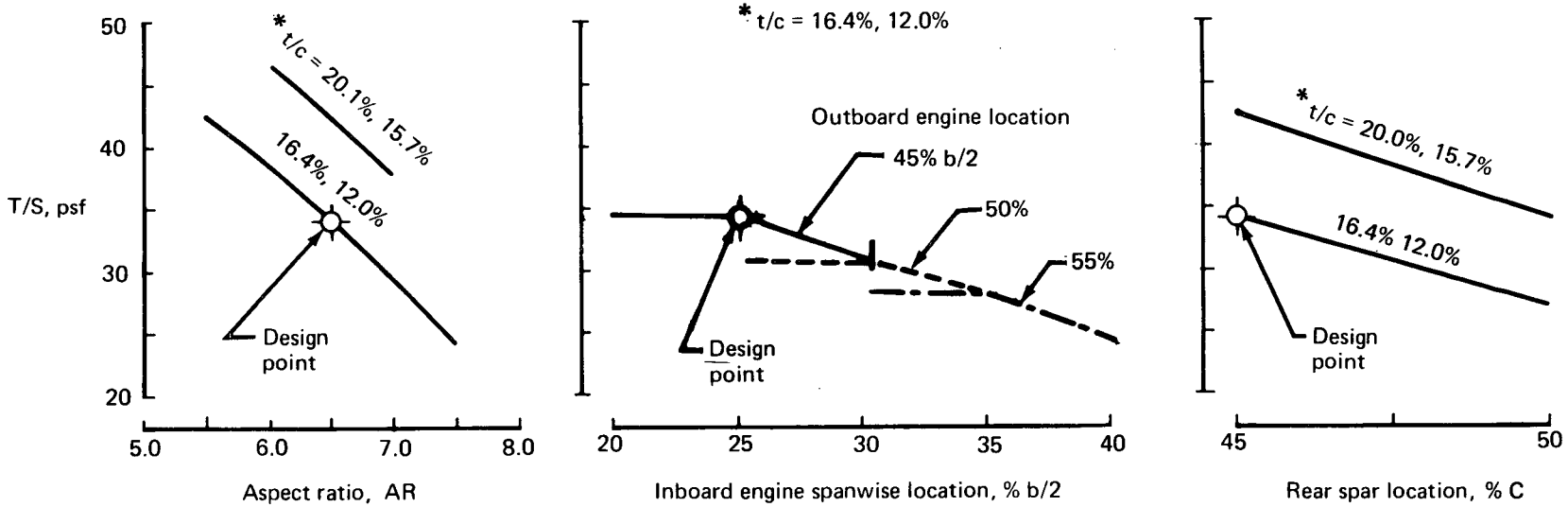

(a) Aspect Ratio

(b) Engine Spanwise Location

(c) Rear Spar Location

*t/c at 11.5% and 50% b/2

FIGURE 10.–EFFECT OF WING GEOMETRY ON THRUST, NPR = 2.6, DUCTING $\Delta P/P_F = 0.14$

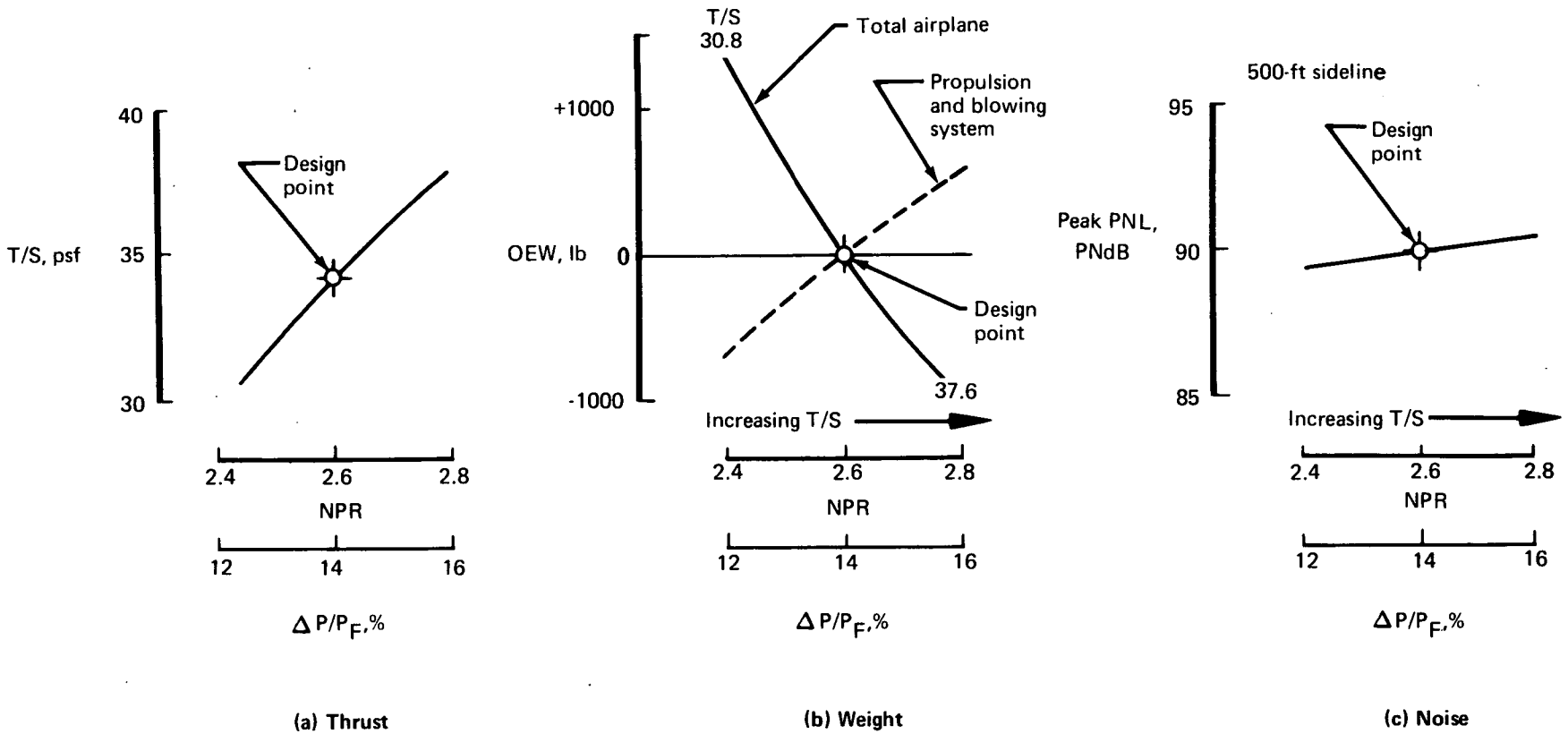

FIGURE 11. –EFFECT OF DUCT FLOW LOSS AND NOZZLE PRESSURE RATIO ON THRUST, WEIGHT, AND NOISE; AR = 6.5

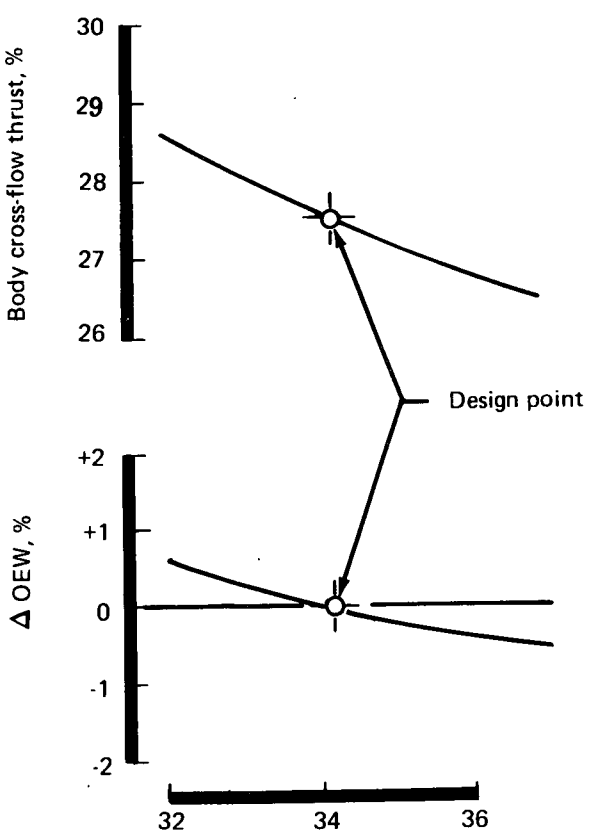

(a) Available Cross-Flow Thrust

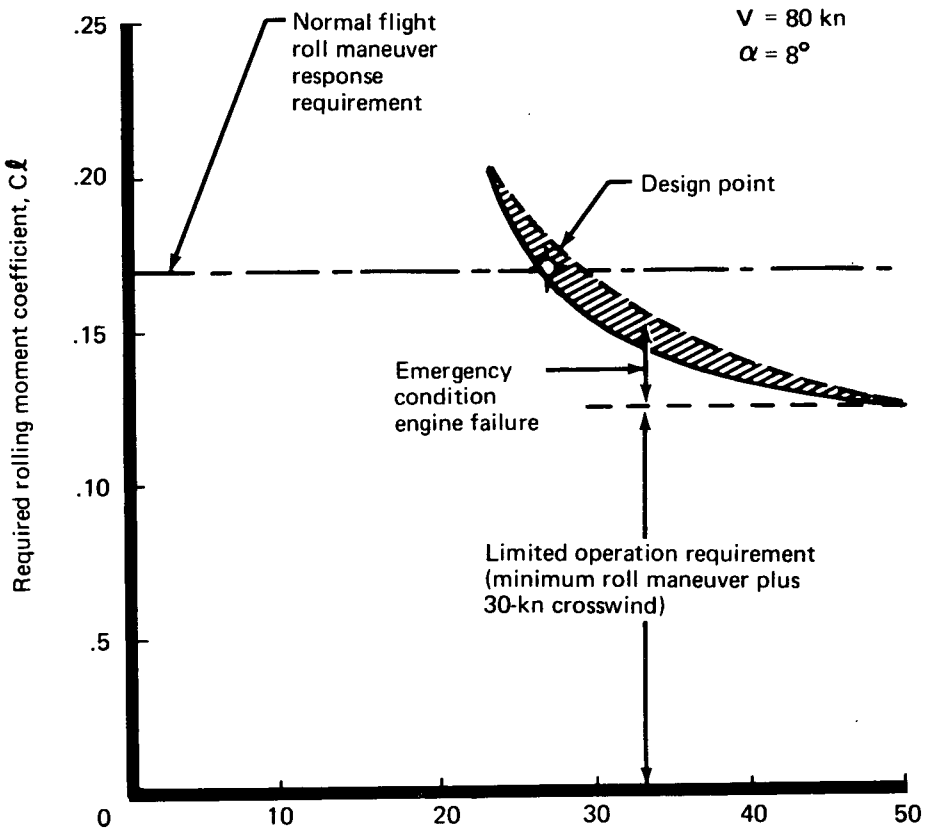

(b) Lateral Control Requirements

FIGURE 12.—CROSS-BODY FLOW REQUIREMENTS, INDEPENDENT DUCT SYSTEM

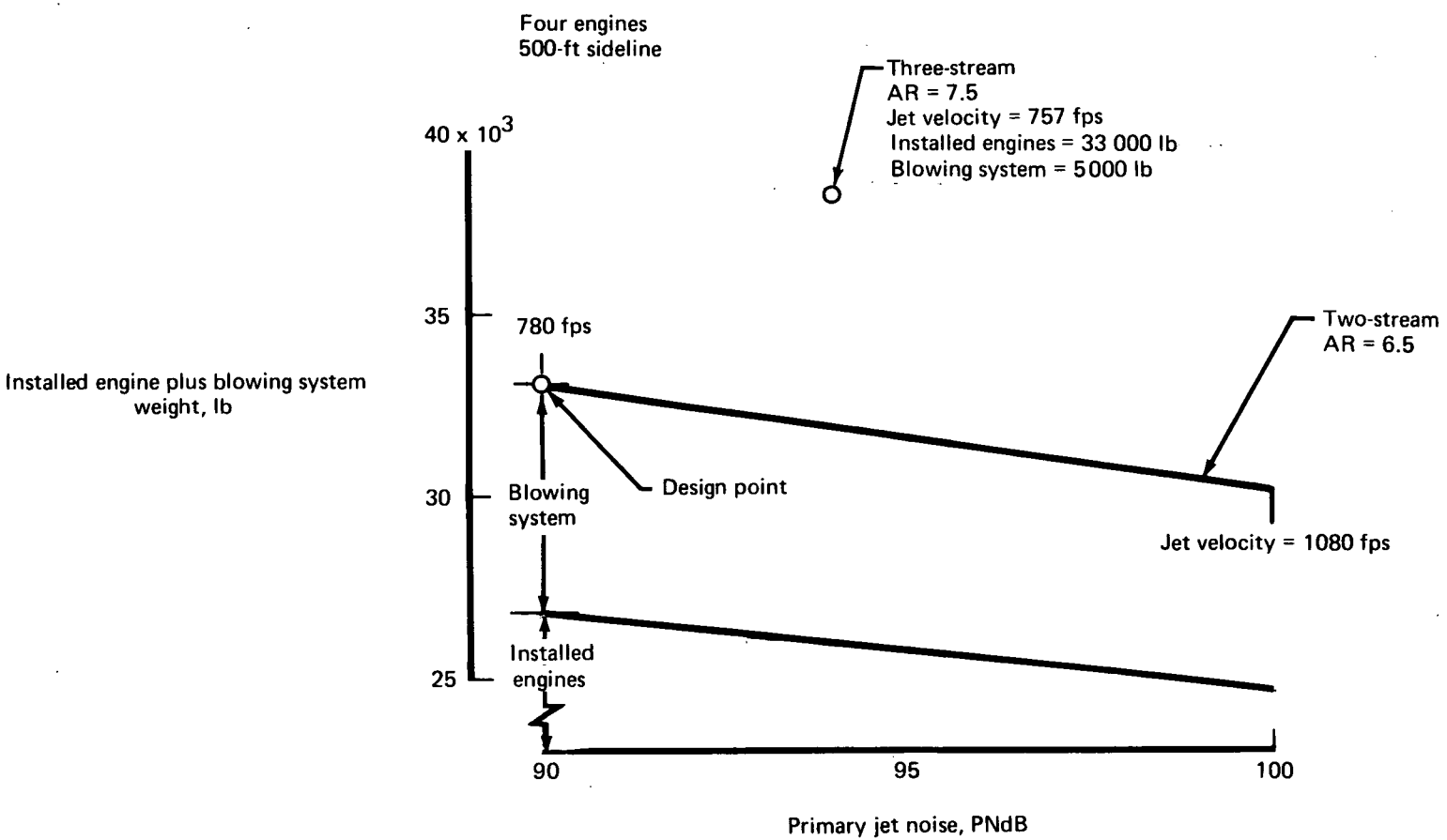

FIGURE 13.–EFFECT OF ENGINE PRIMARY JET VELOCITY ON WEIGHT AND NOISE

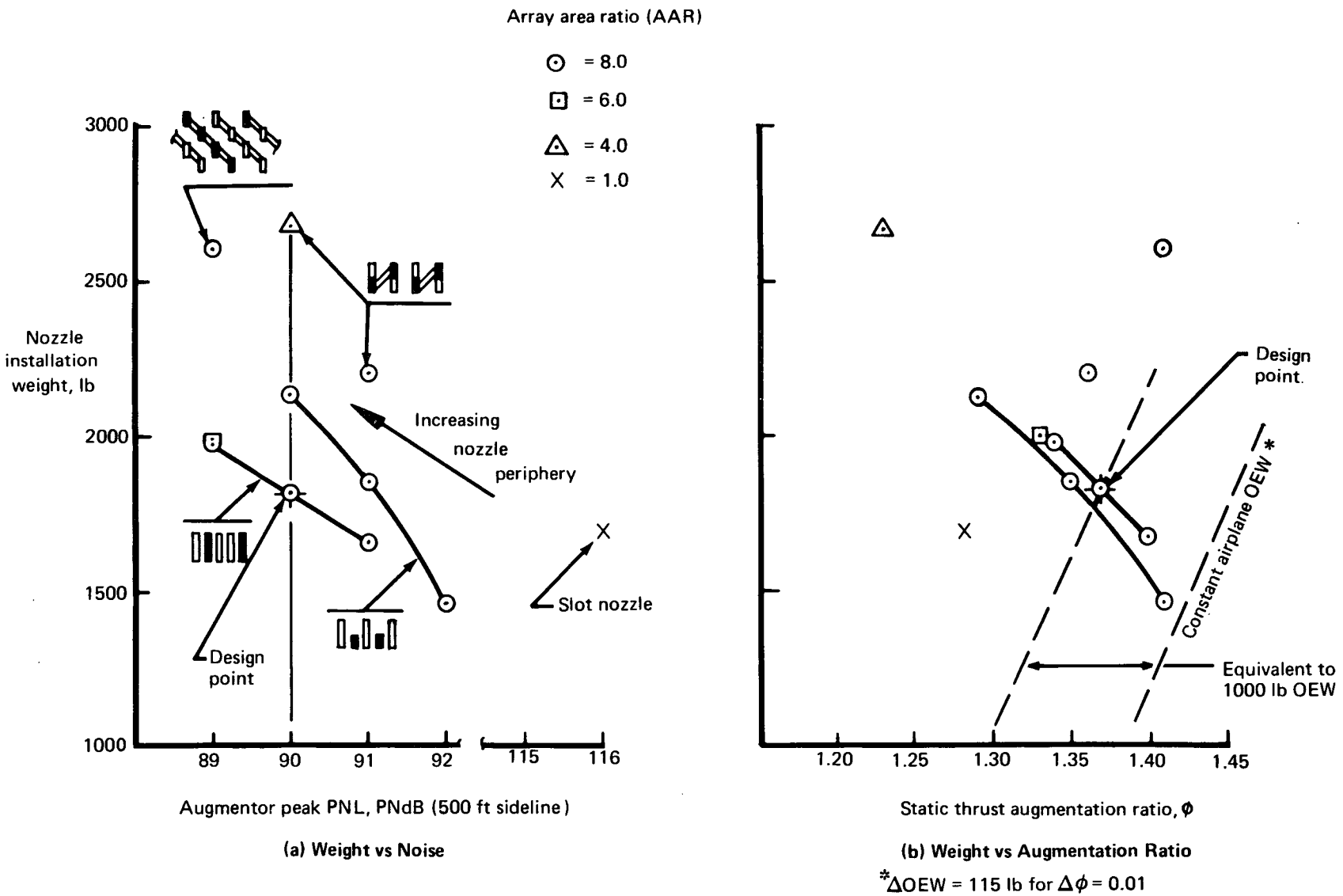

FIGURE 14.—EFFECT OF AUGMENTOR NOZZLE CONFIGURATION ON NOISE, AUGMENTATION RATIO, AND WEIGHT; 1978 AIRPLANE

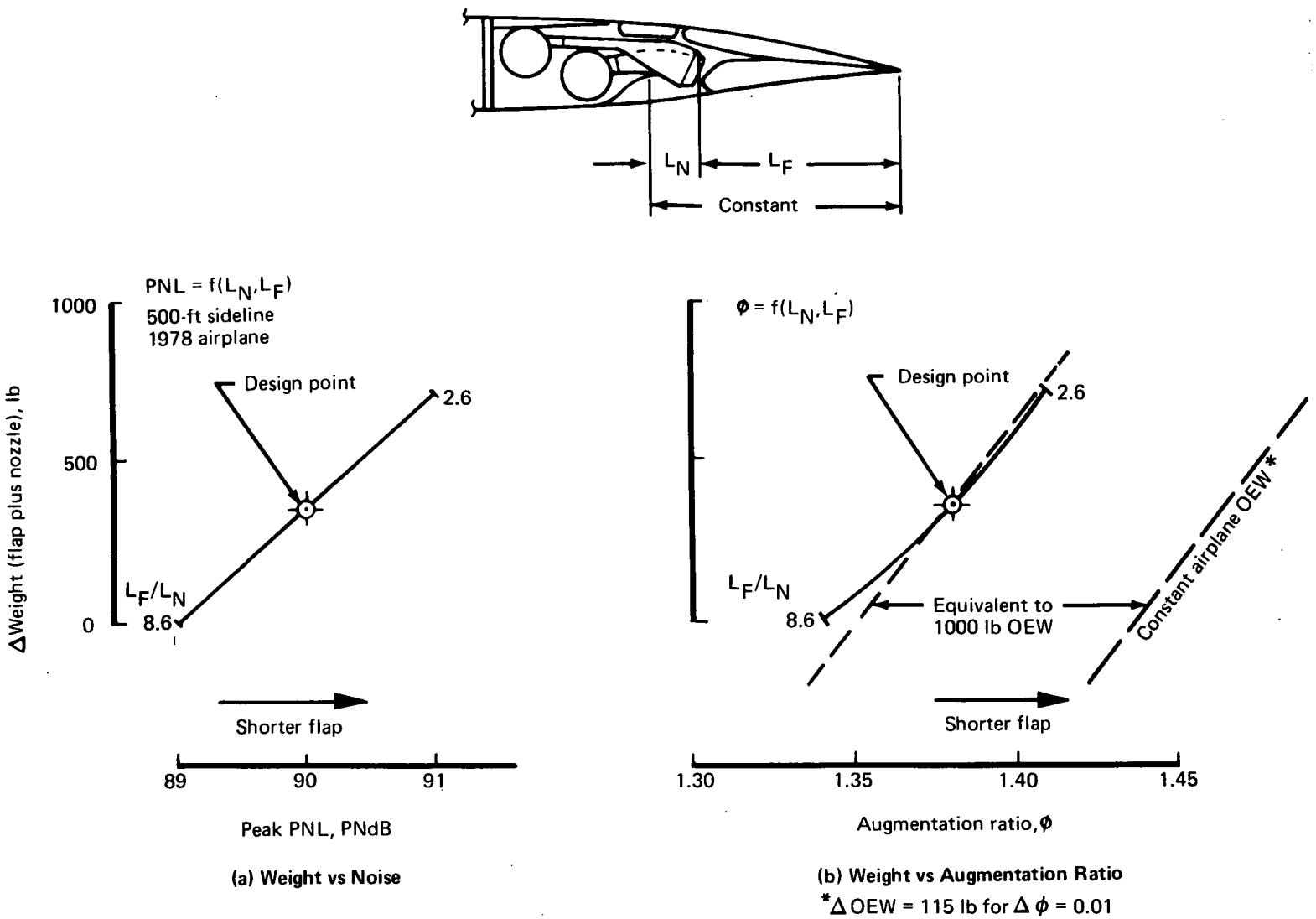

FIGURE 15.–EFFECT OF NOZZLE AND FLAP LENGTHS ON NOISE, AUGMENTATION RATIO, AND WEIGHT; 1978 AIRPLANE

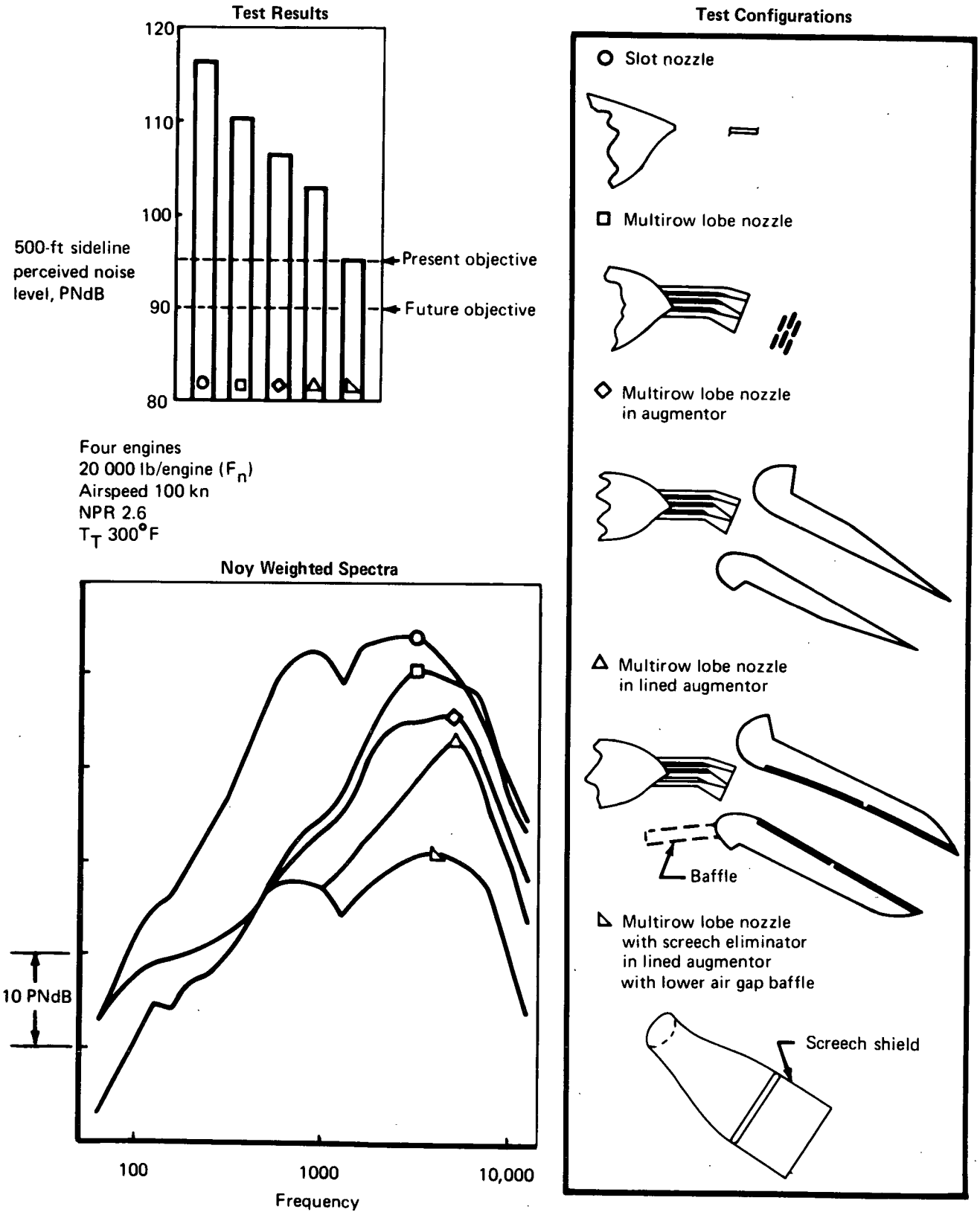

FIGURE 16.–TAKEOFF PERCEIVED NOISE LEVELS

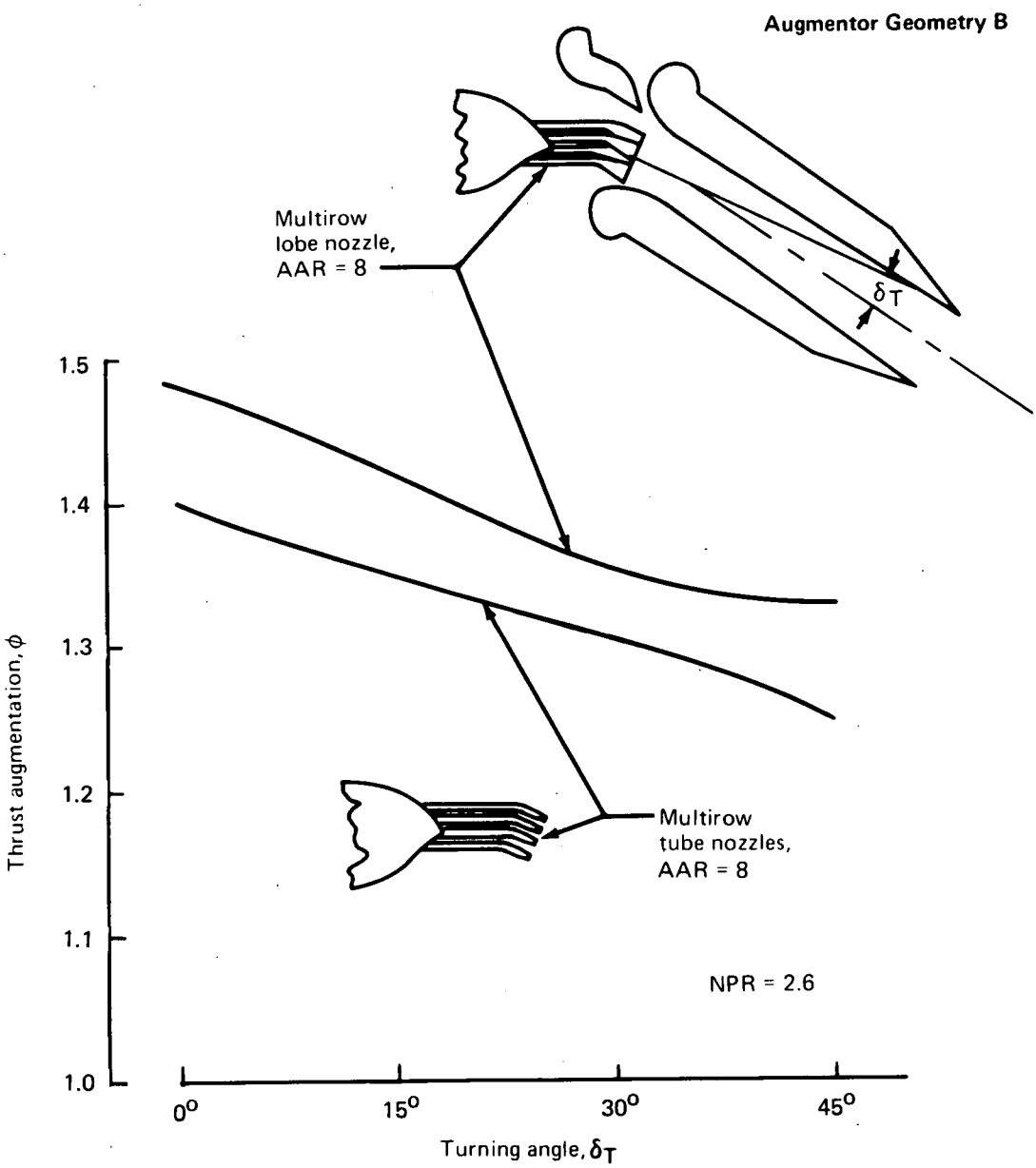

FIGURE 17.–AUGMENTOR FLOW TURNING PERFORMANCE

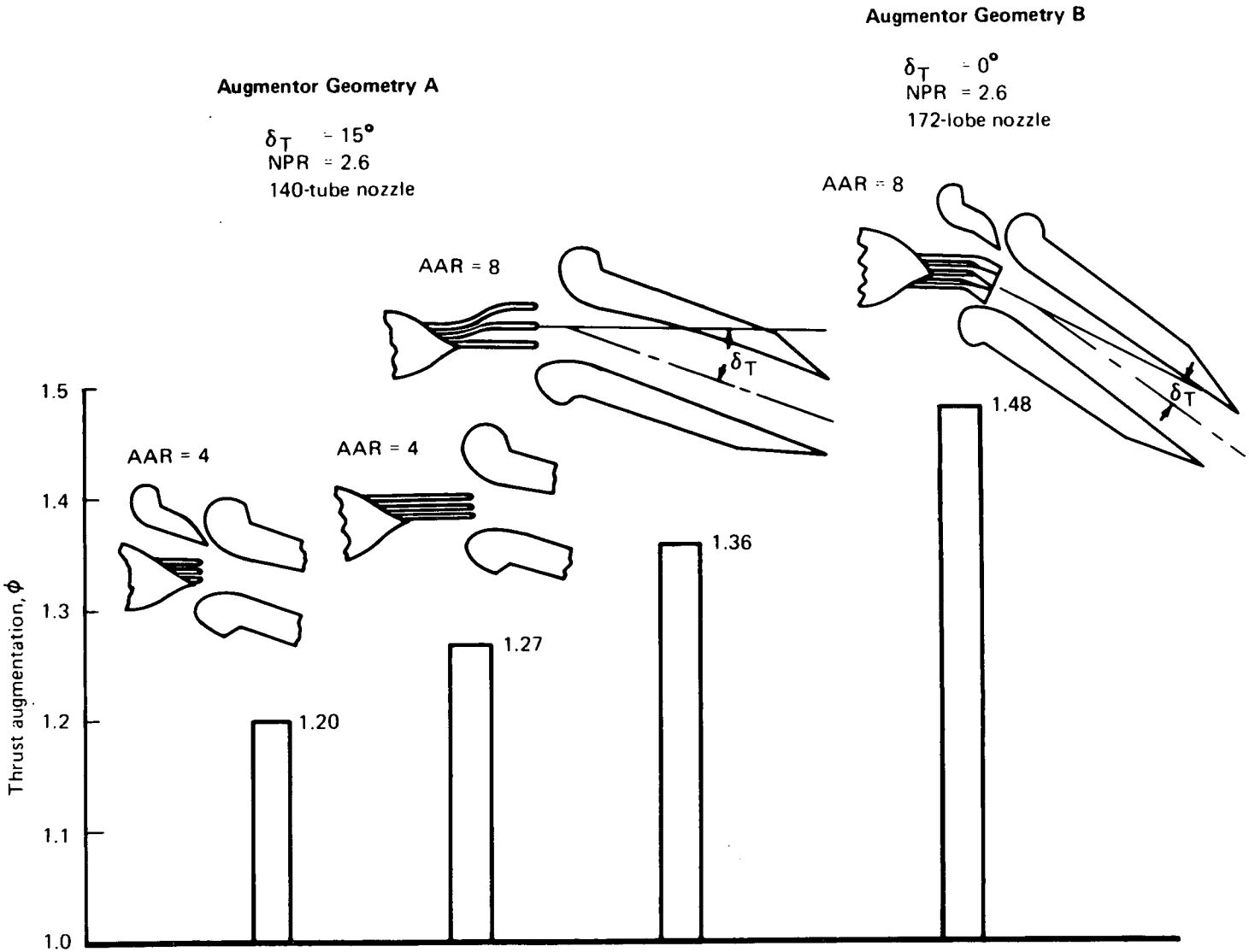

FIGURE 18.–PRIMARY NOZZLE GEOMETRY EFFECTS

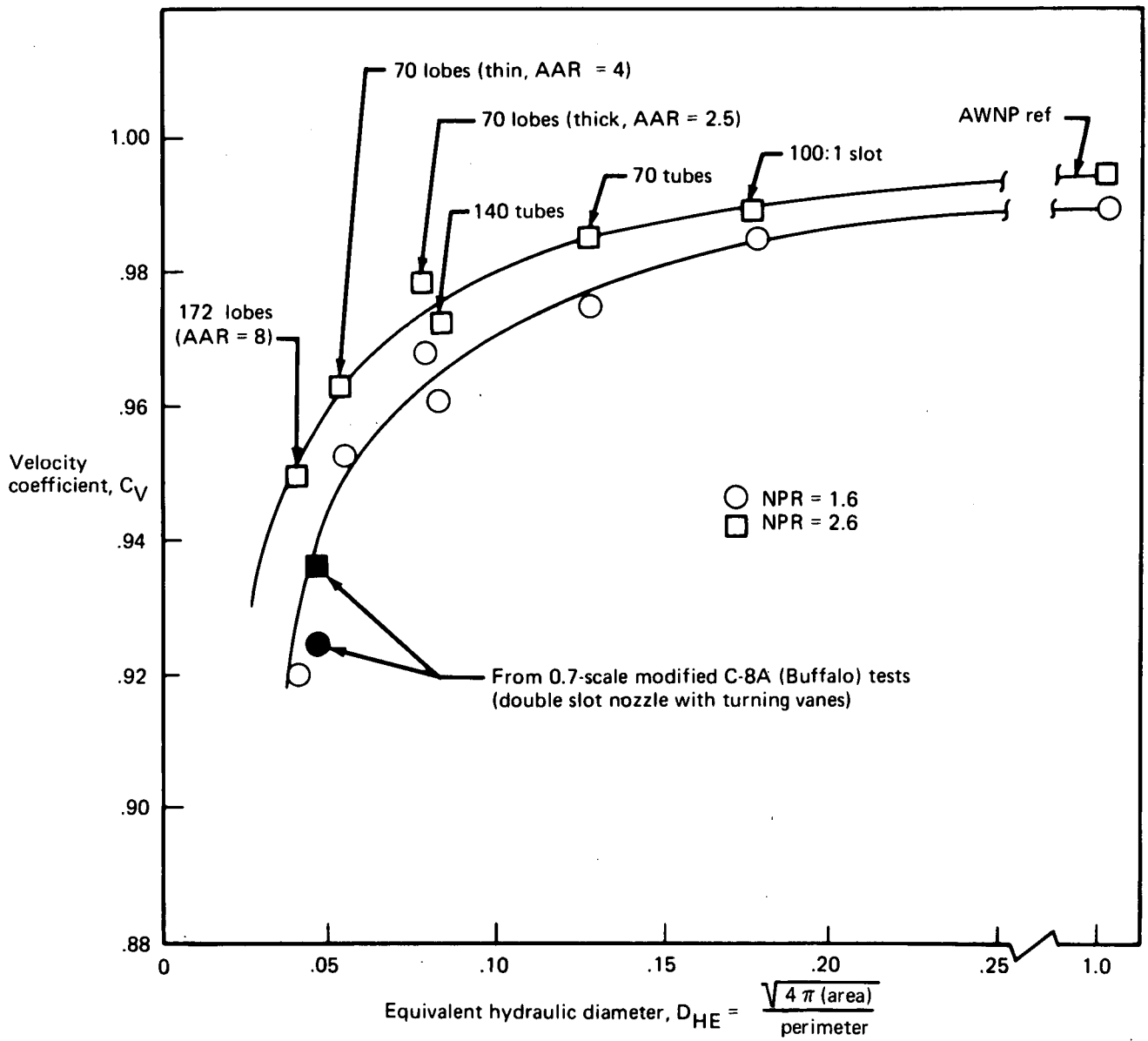

FIGURE 19.–CORRELATION OF NOZZLE PERFORMANCE

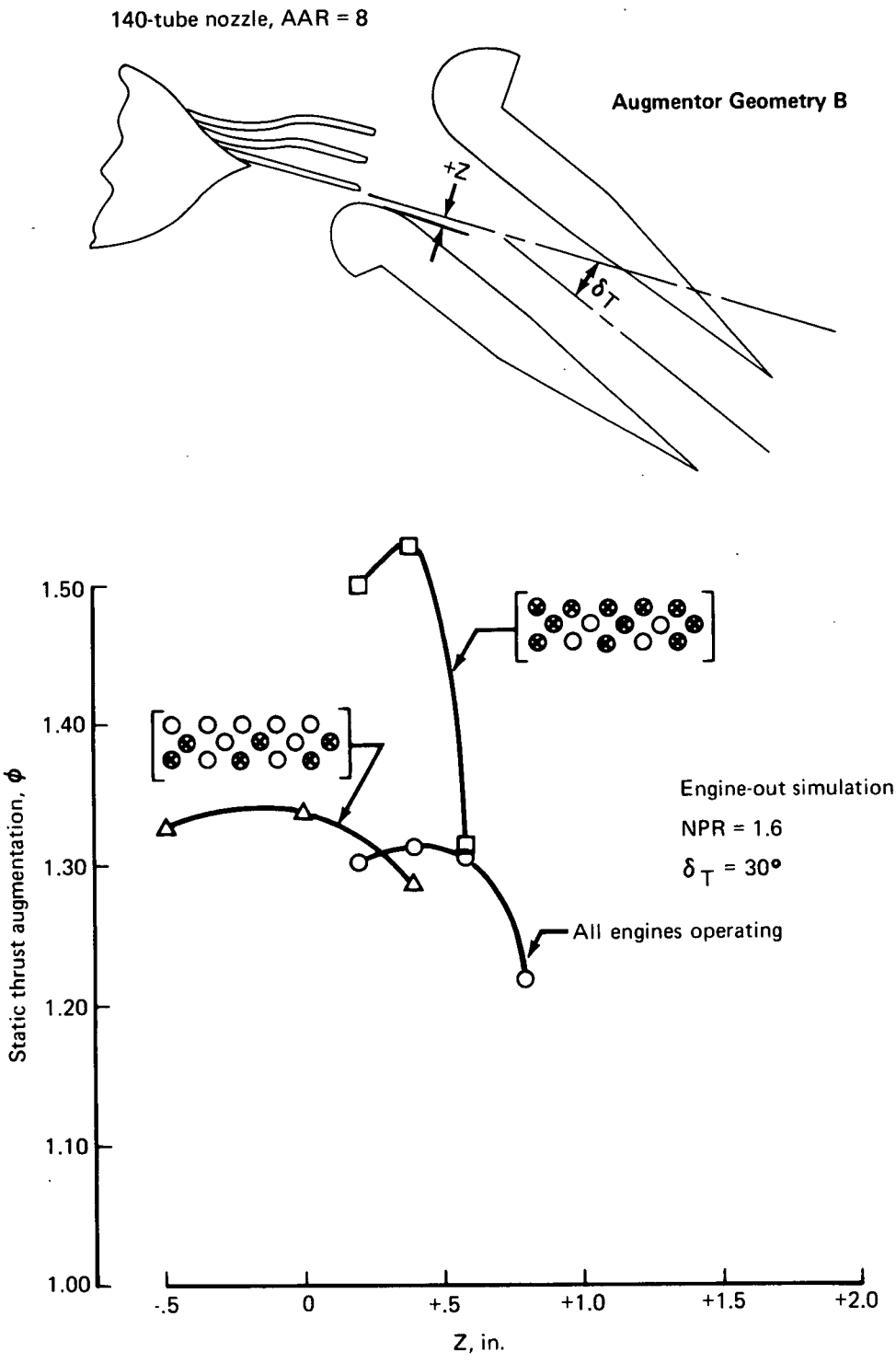

FIGURE 20.—ENGINE-OUT SIMULATION, APPROACH CONDITION

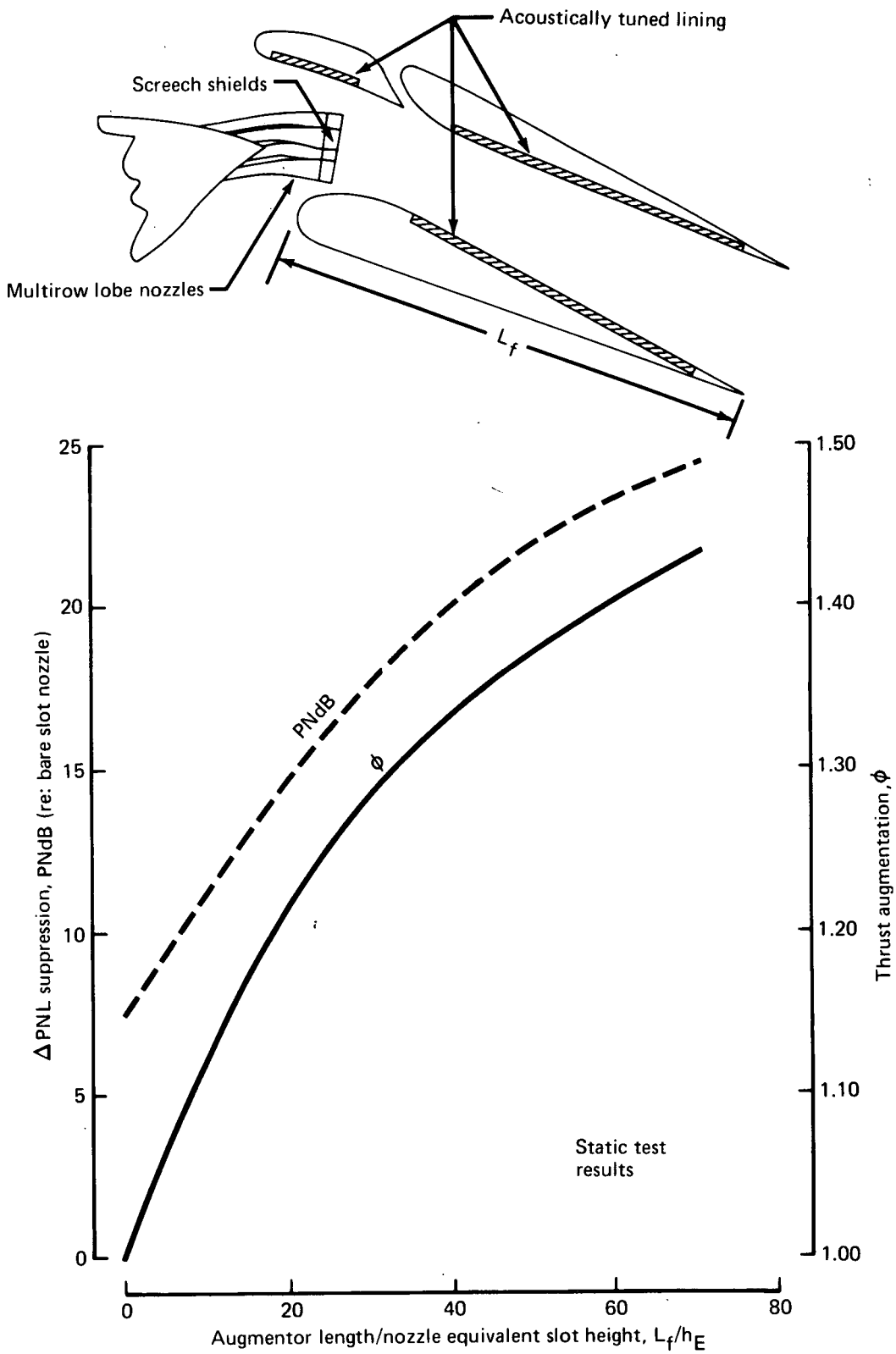

FIGURE 21.—AUGMENTOR LENGTH EFFECTS

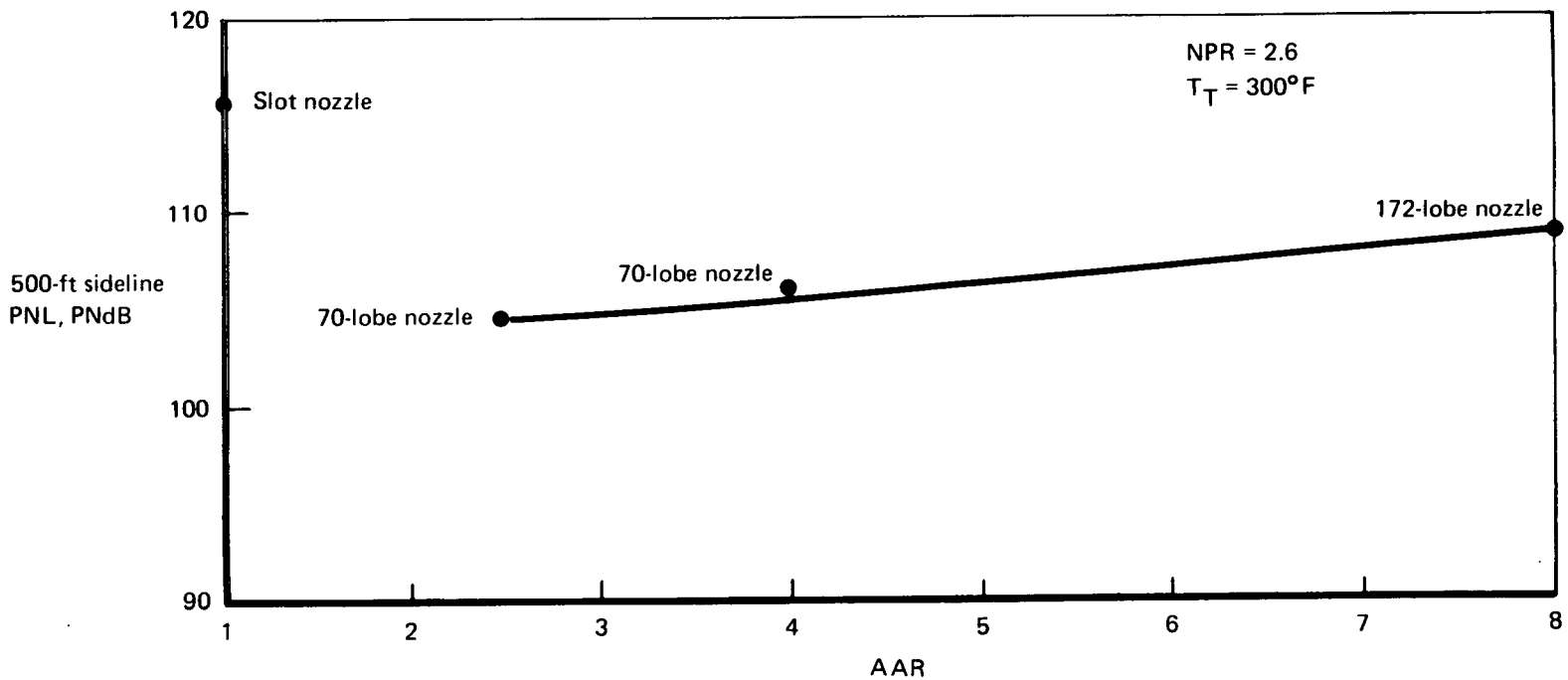

FIGURE 22.–EFFECT OF NOZZLE ARRAY AREA RATIO ON PERCEIVED NOISE LEVEL, AUGMENTOR PRIMARY NOZZLE ONLY

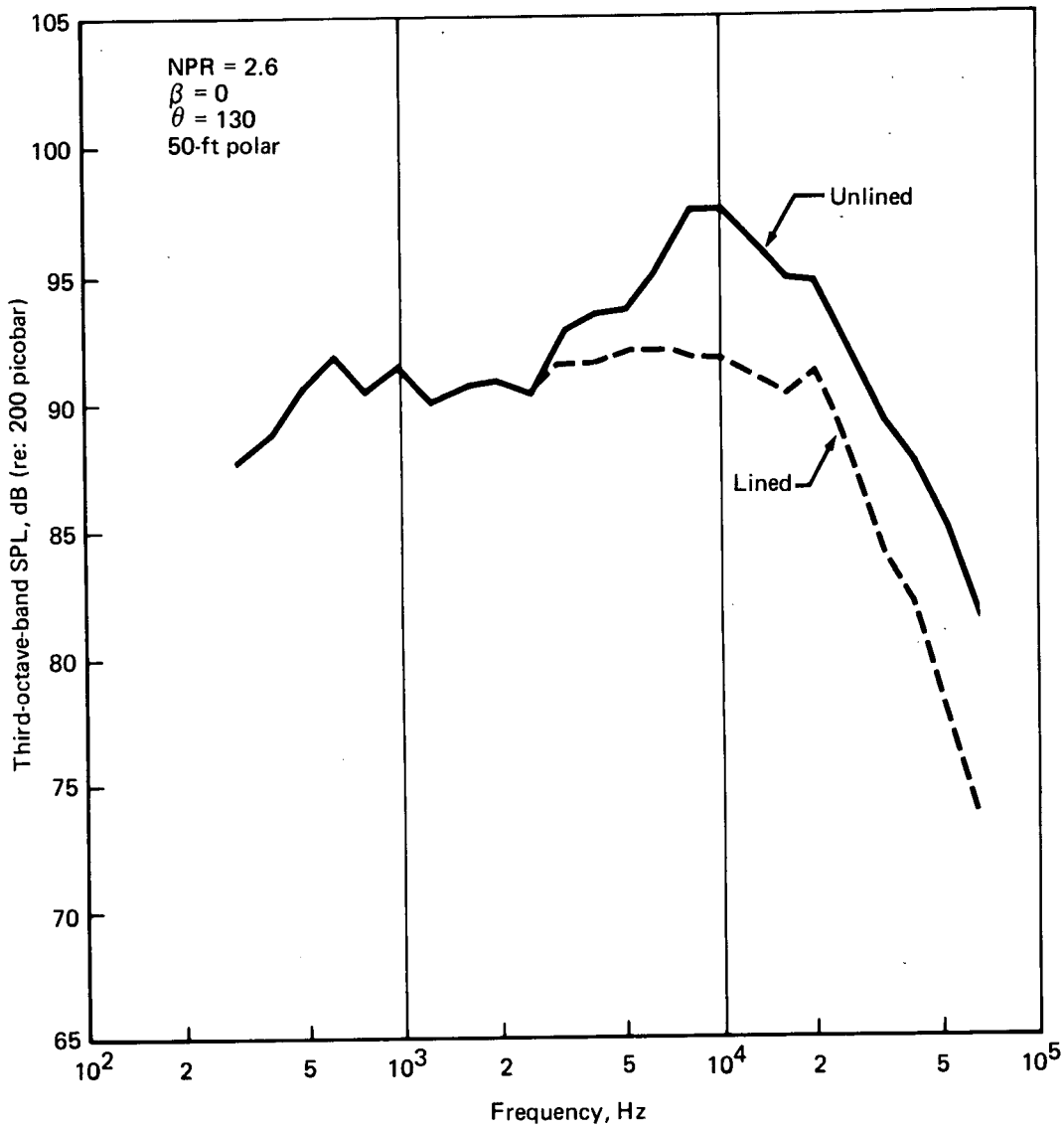

FIGURE 23.—COMPARISON OF NOISE SPECTRA, UNLINED VS LINED AUGMENTOR, AS MEASURED, MODEL SCALE (70-LOBE NOZZLE, LINING 11B)

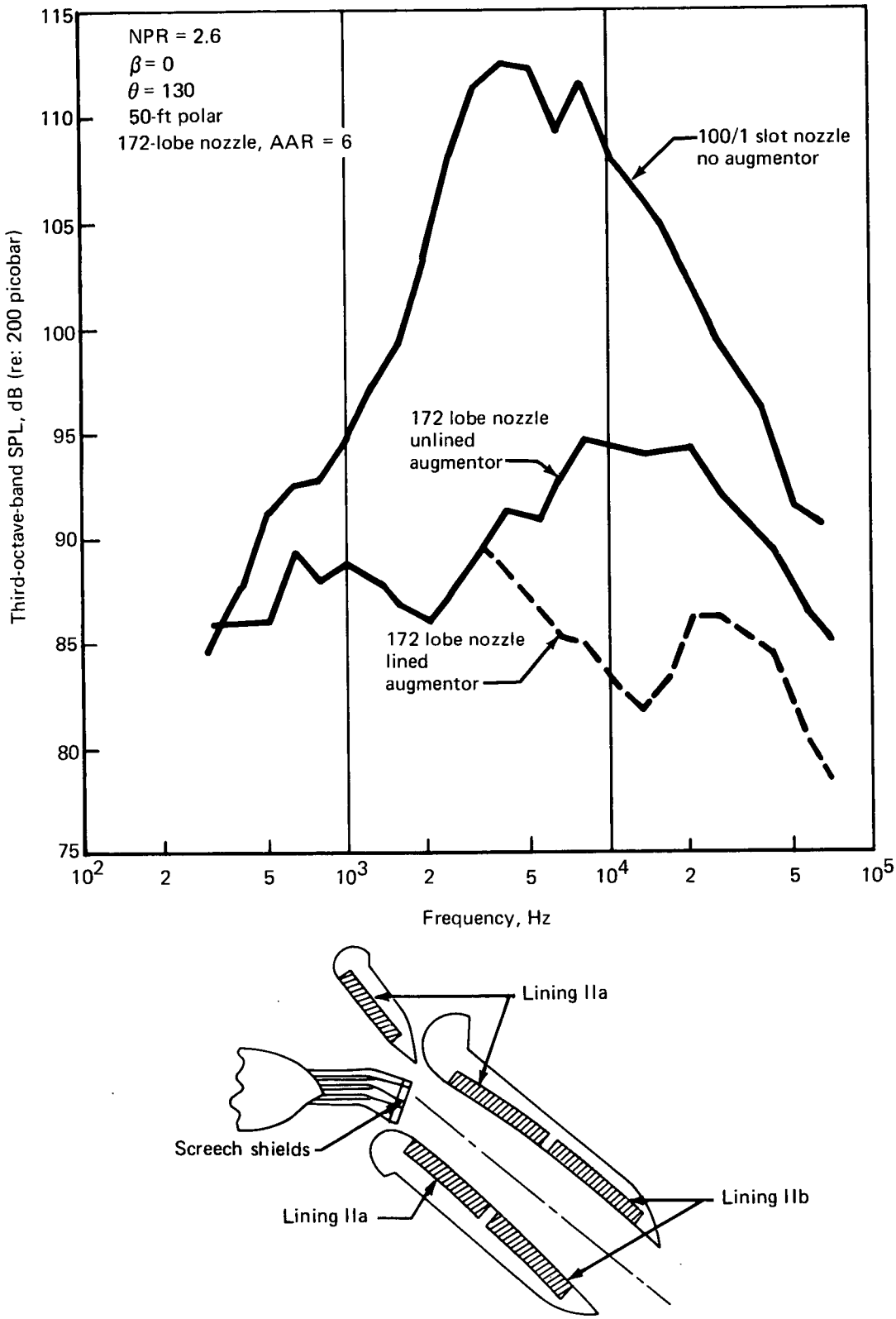

FIGURE 24.–COMPARISON OF NOISE SPECTRA, UNLINED AND LINED AUGMENTOR WITHOUT SCREECH VS 100/1 SLOT NOZZLE, AS MEASURED, MODEL SCALE

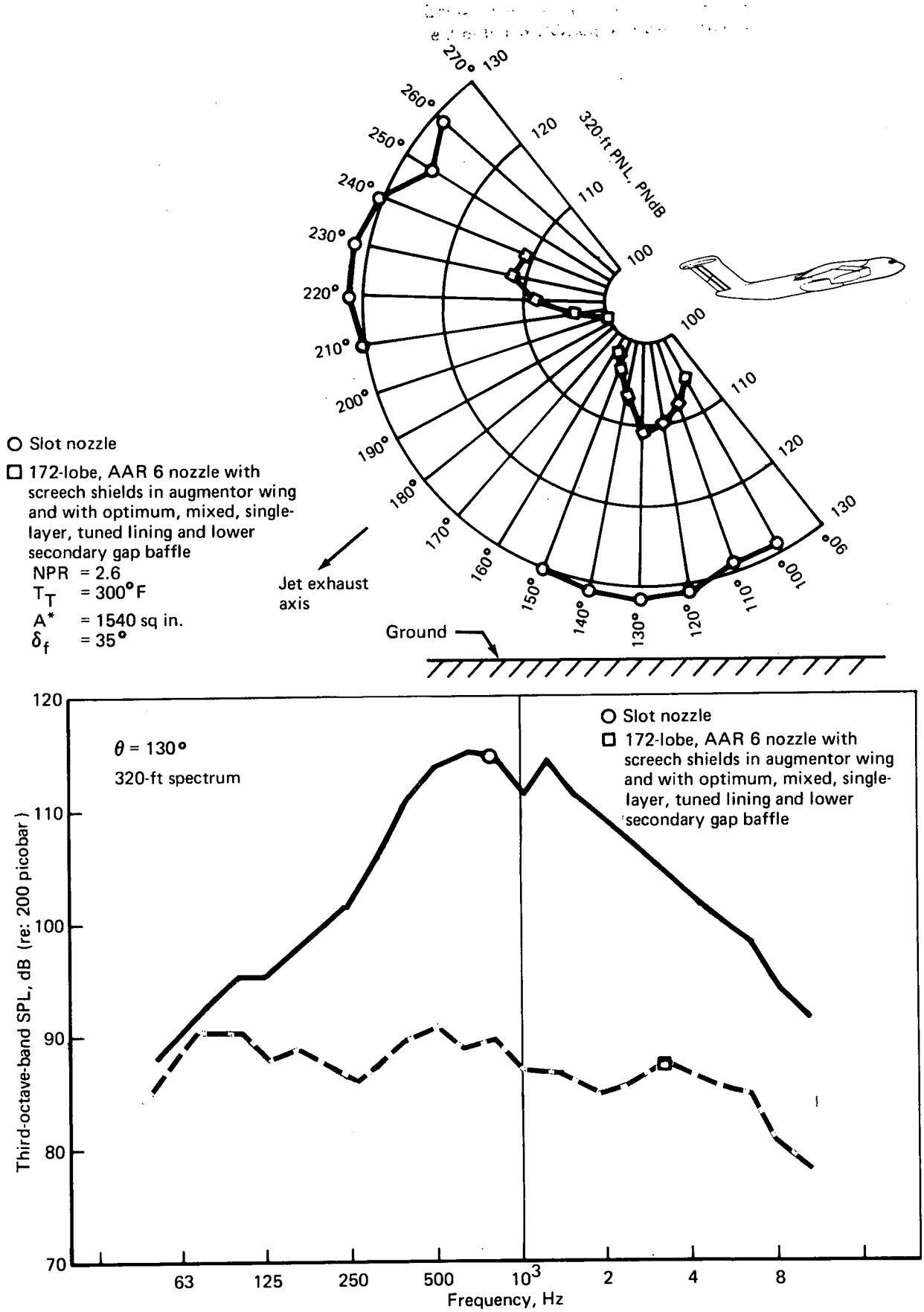

FIGURE 25.—21-PNdB SUPPRESSOR SPECTRA AND BEAM PATTERNS; 150 PASSENGERS, FOUR ENGINES, 20 000 LB THRUST EACH

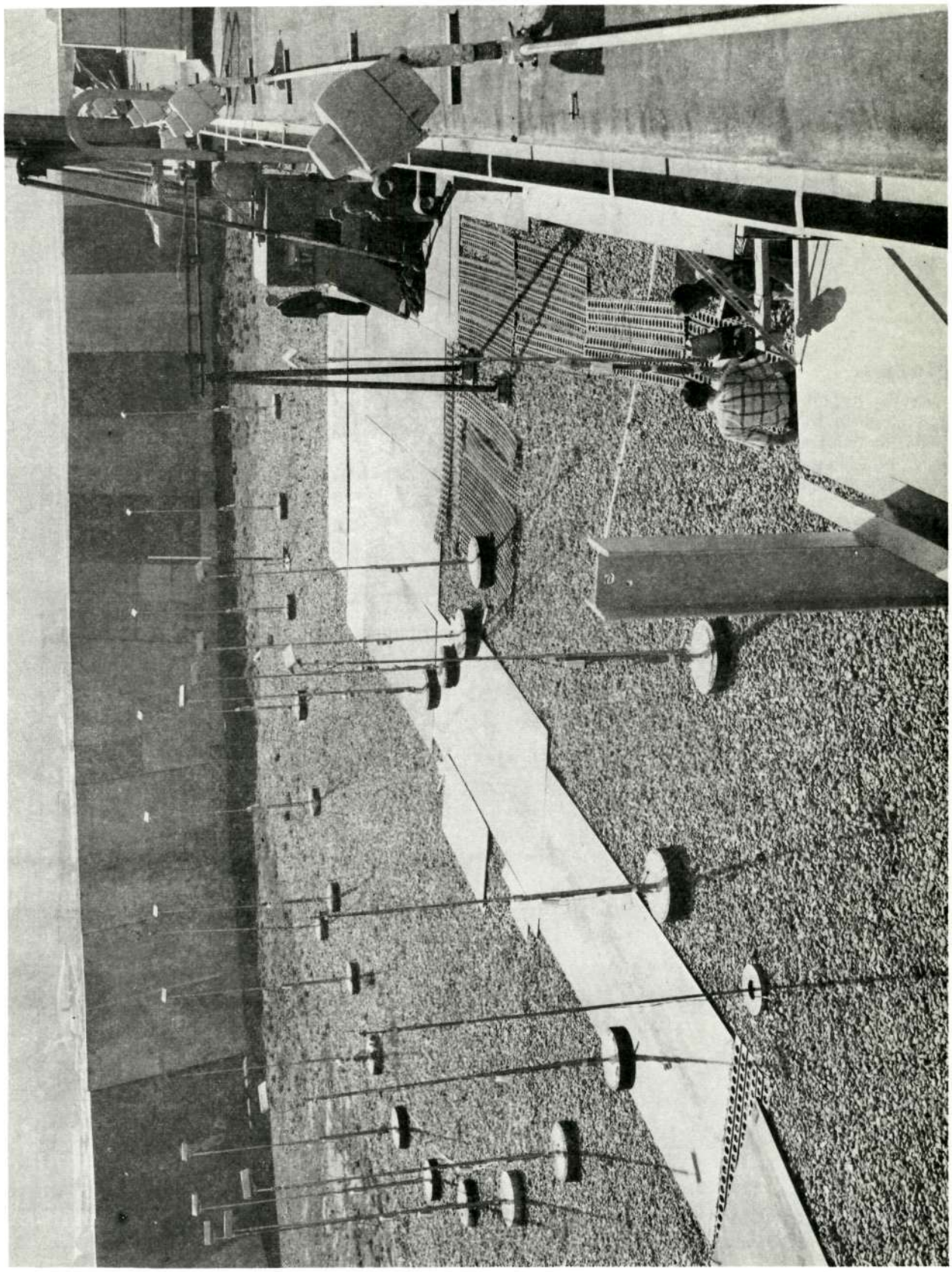

FIGURE 26.—STATIC TEST FACILITY ACOUSTIC ARENA

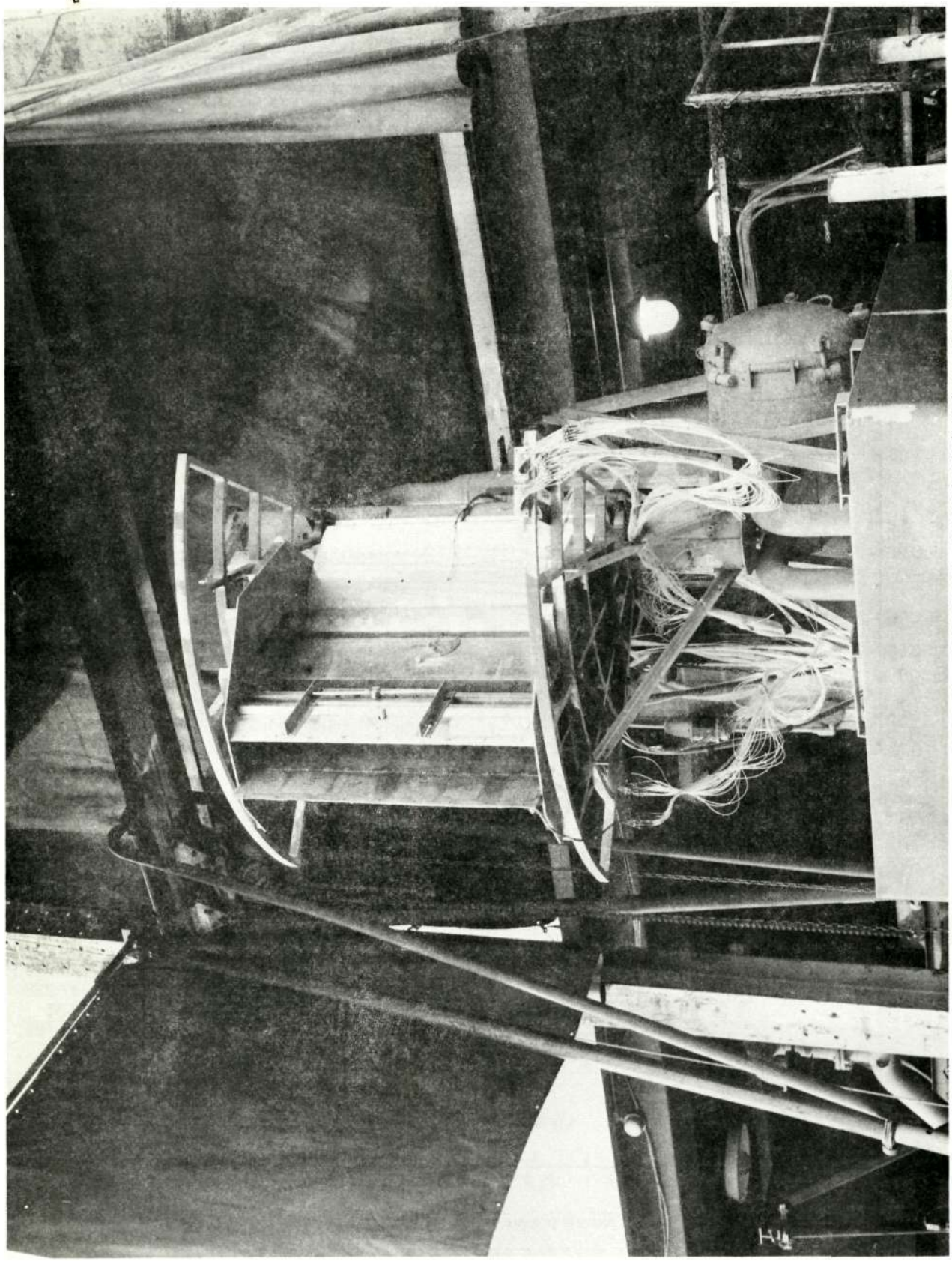

FIGURE 27.—AUGMENTOR FLAP MODEL IN STATIC TEST FACILITY

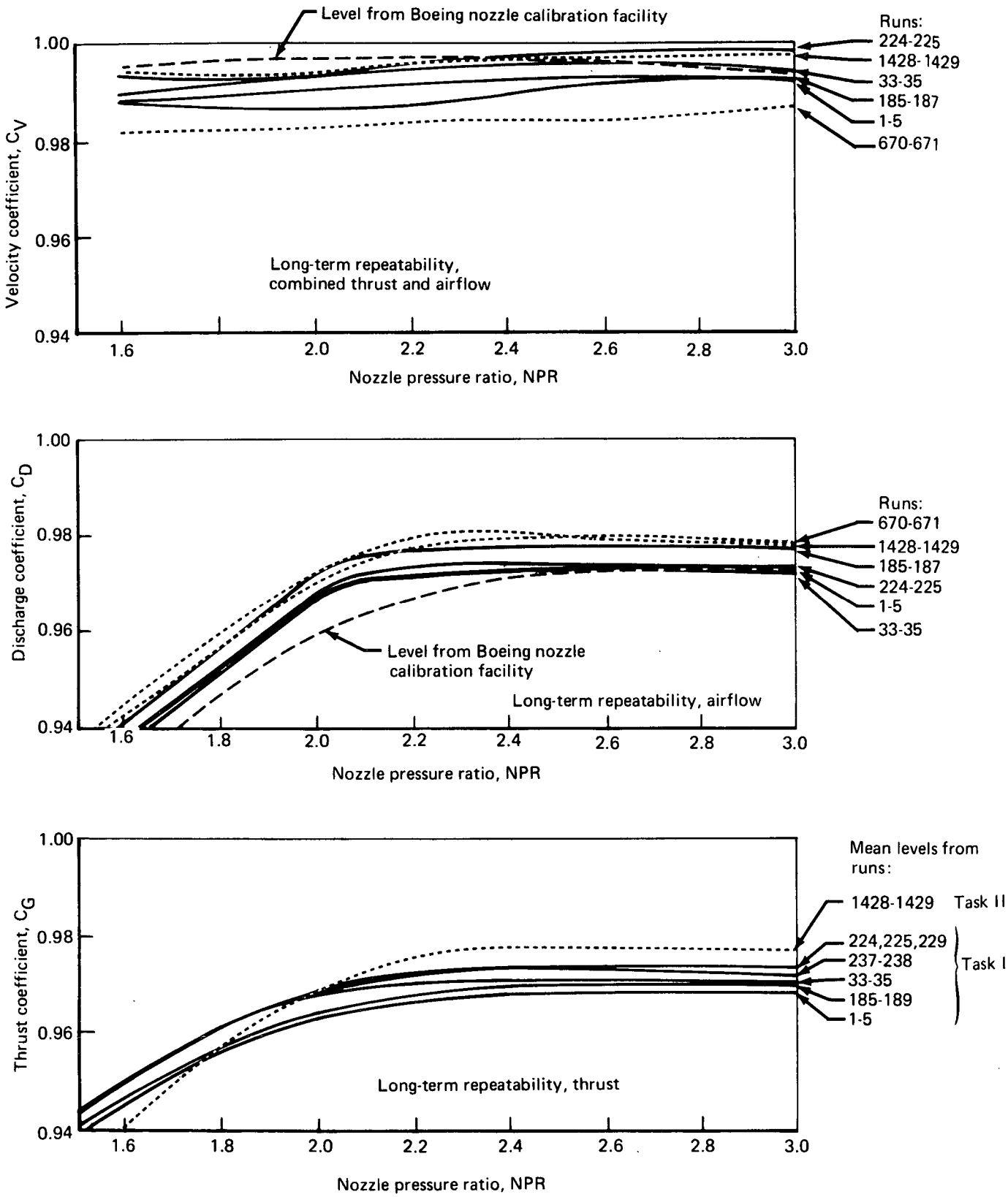

FIGURE 28.– REFERENCE NOZZLE PERFORMANCE REPEATABILITY

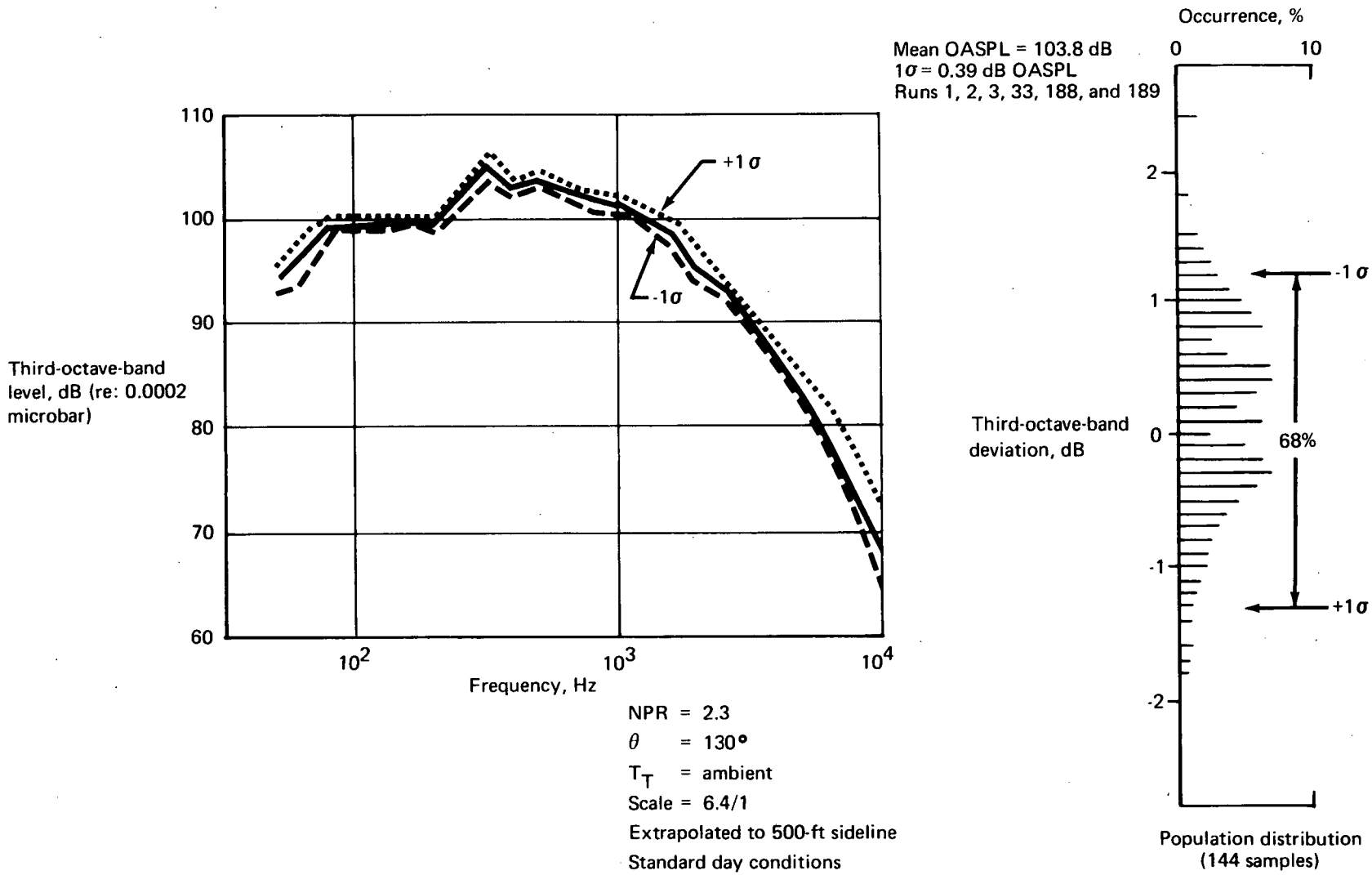

FIGURE 29.--ROUND CONVERGENT NOZZLE MEAN SPECTRUM WITH STANDARD DEVIATIONS

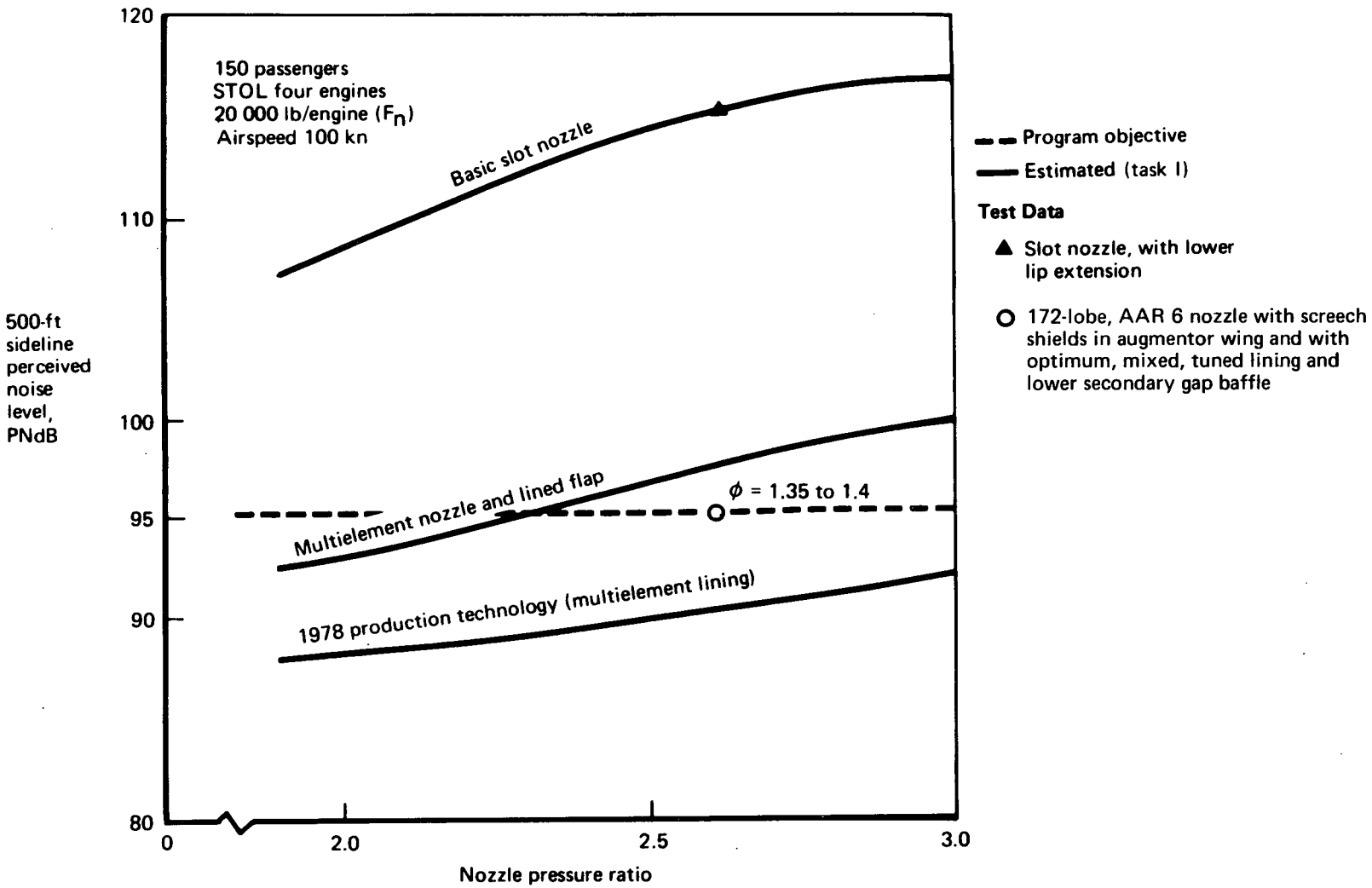

FIGURE 30. – AUGMENTOR WING NOISE LEVELS

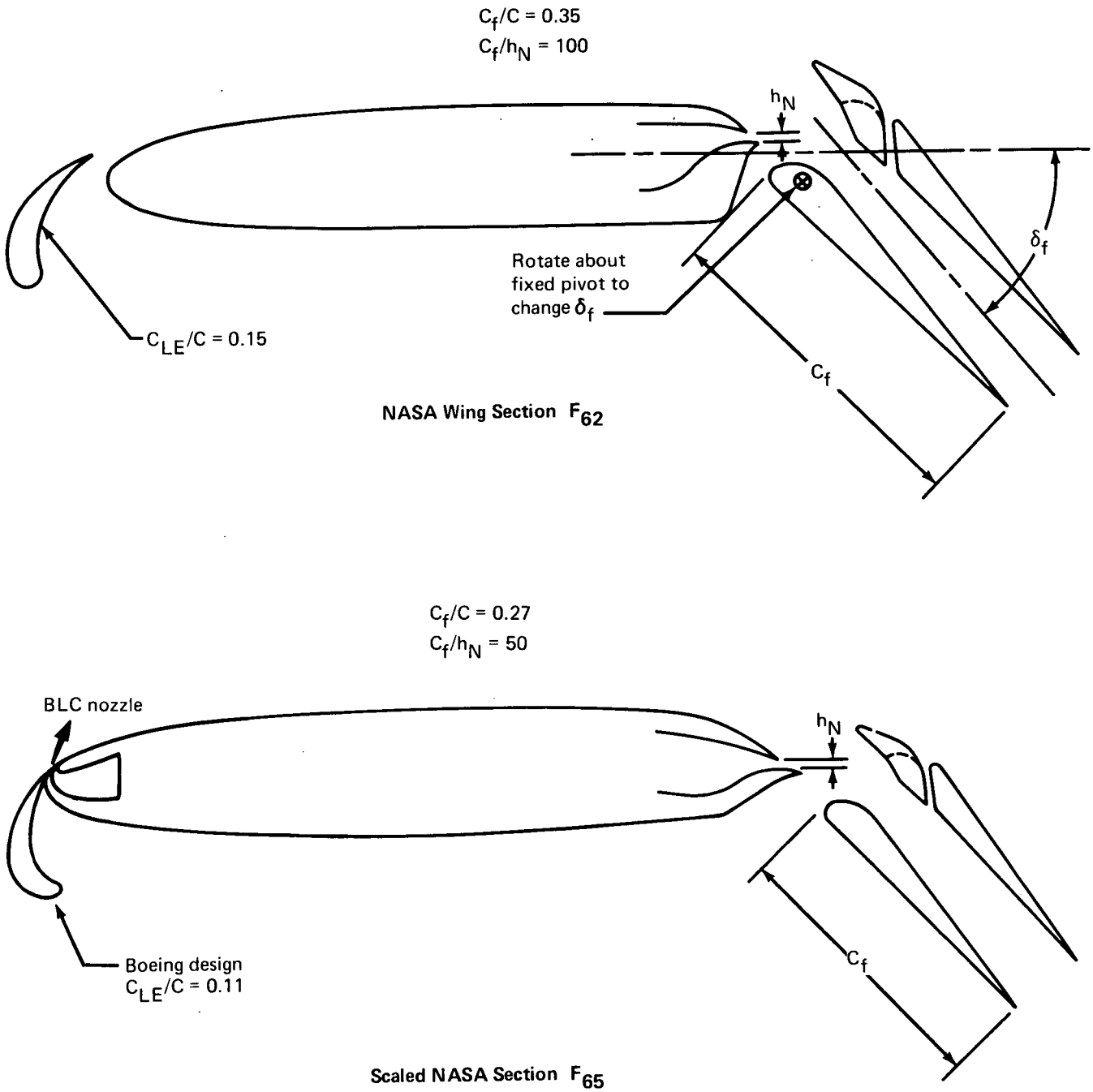

FIGURE 31.–SLOT NOZZLE CONFIGURATIONS TESTED

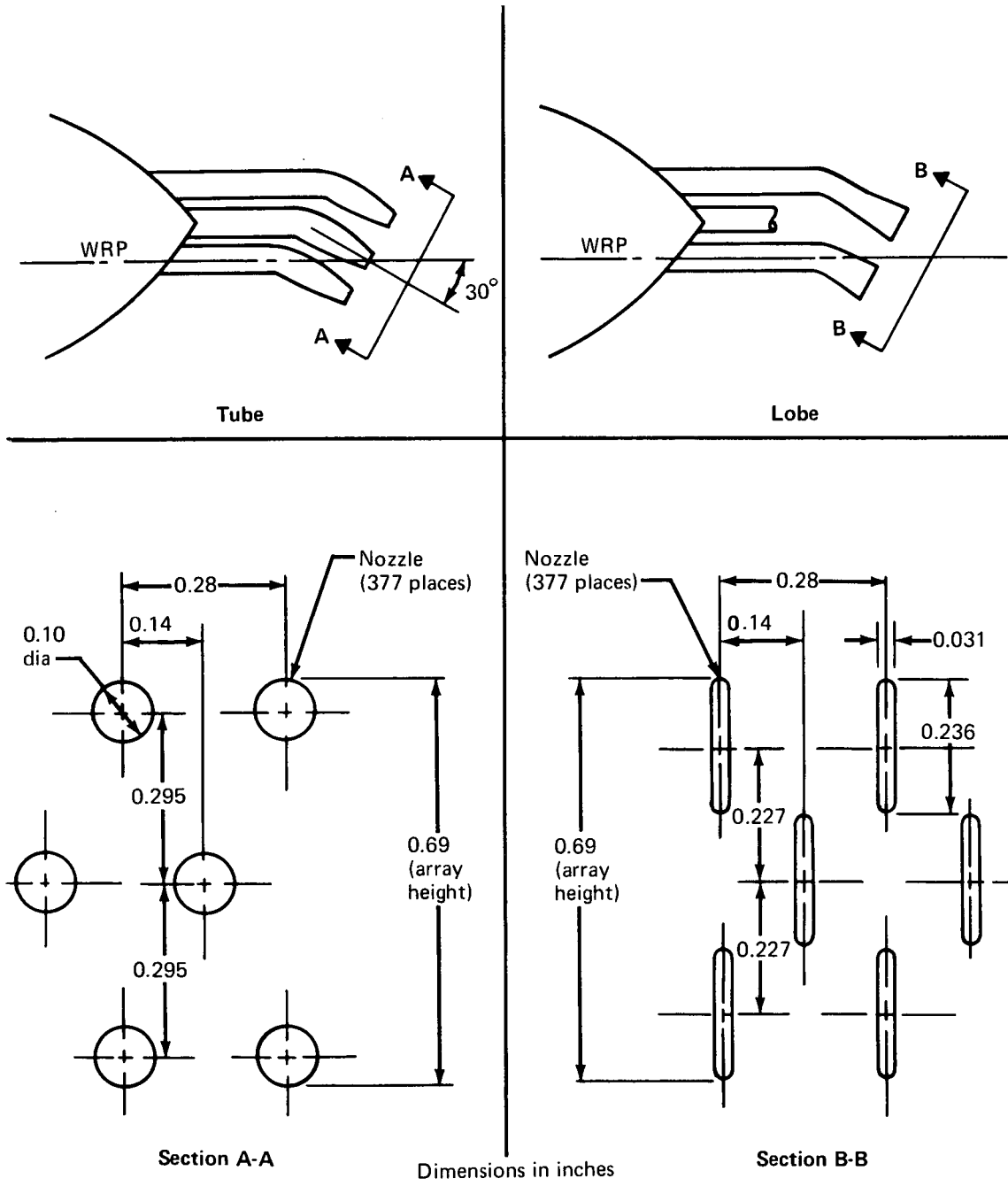

FIGURE 32.–MULTIELEMENT NOZZLE ARRANGEMENT

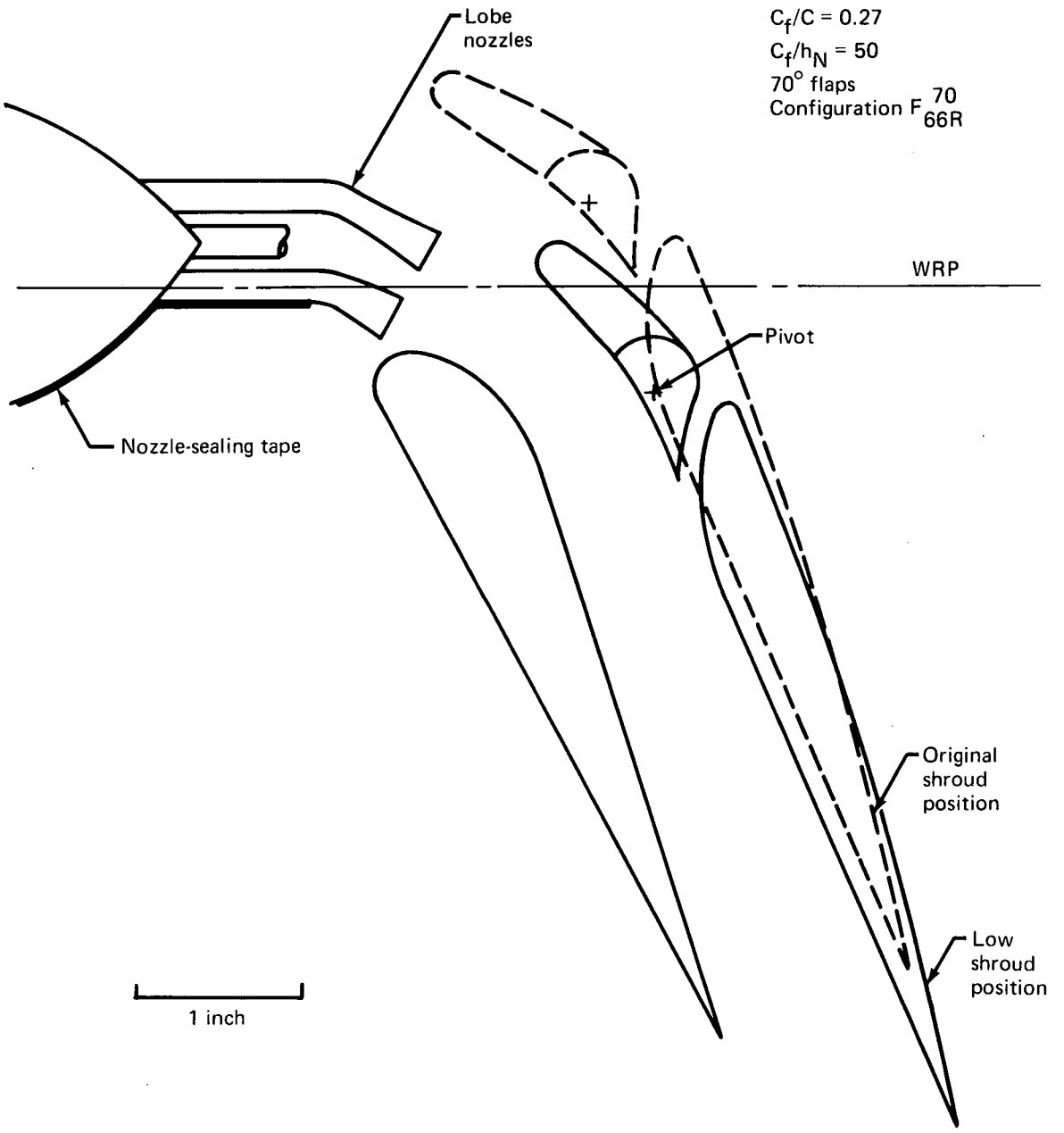

FIGURE 33.–MULTILOBE AUGMENTOR FLAP, OPTIMUM FLAP GEOMETRY FOR $\delta_f = 70°$

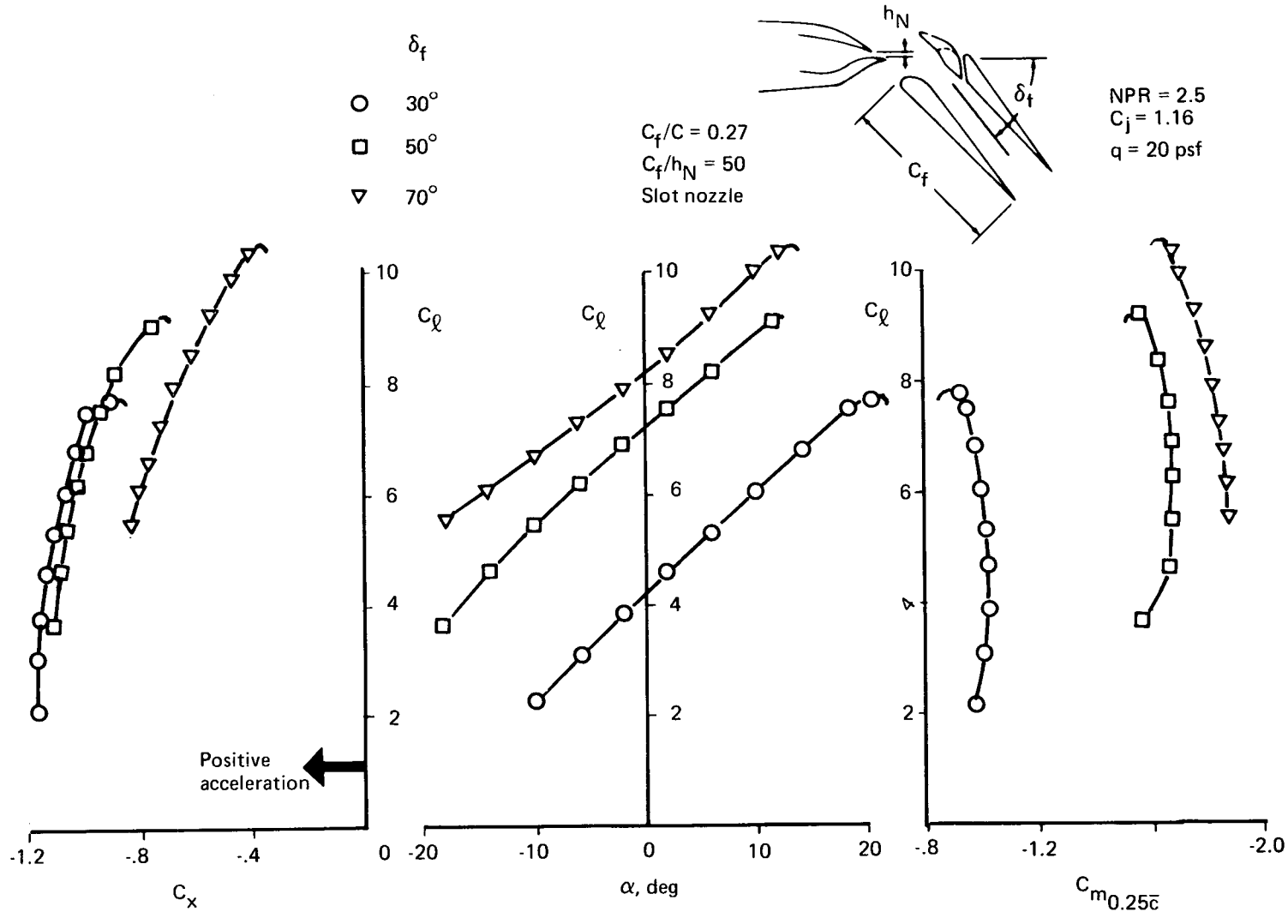

FIGURE 34.—REPRESENTATIVE AERODYNAMIC DATA FOR THE SCALED NASA SECTION AT $C_j = 1.16$

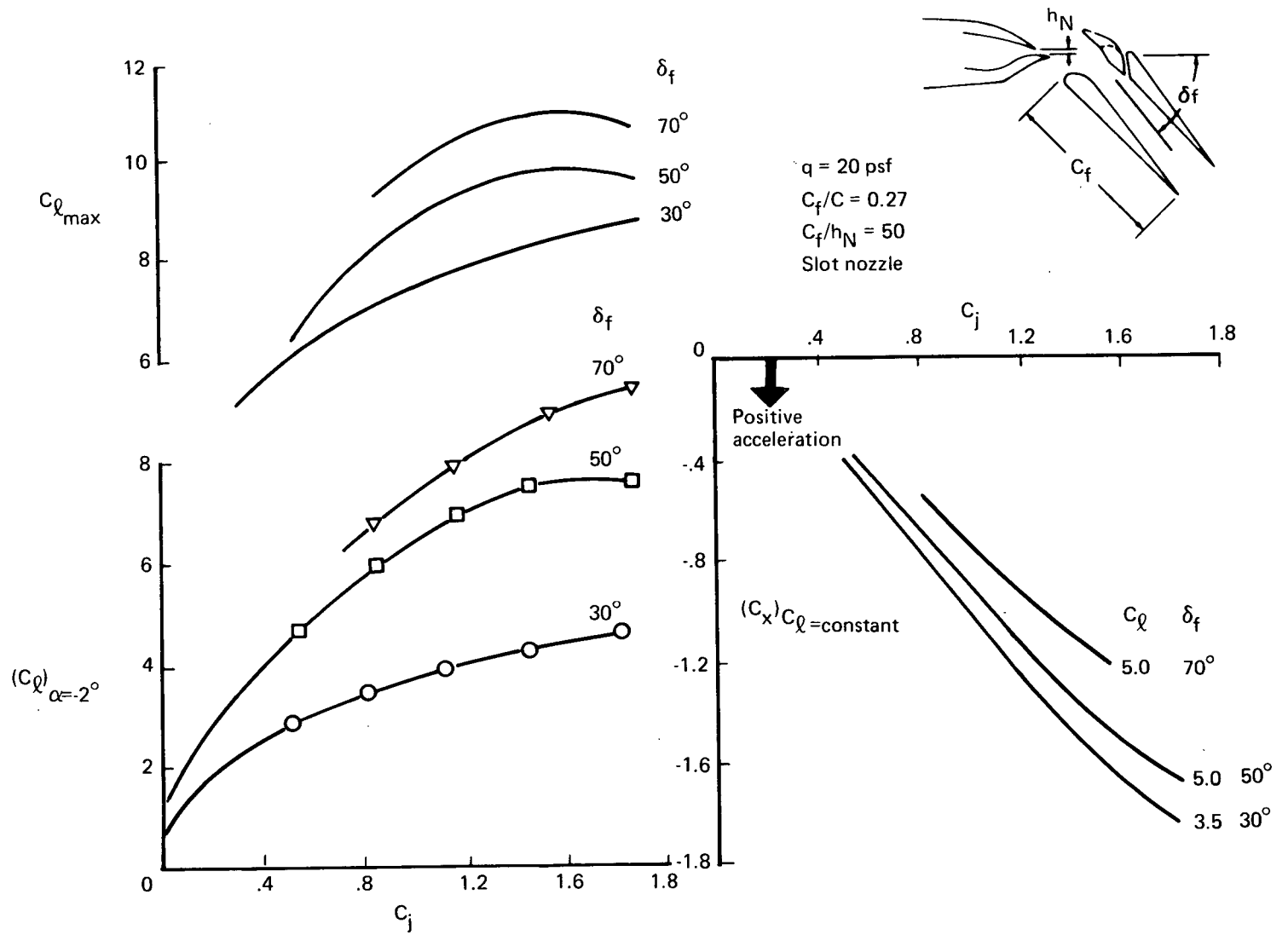

FIGURE 35.—VARIATION OF LIFT AND STREAMWISE FORCE WITH C_j FOR THE SCALED NASA SECTION

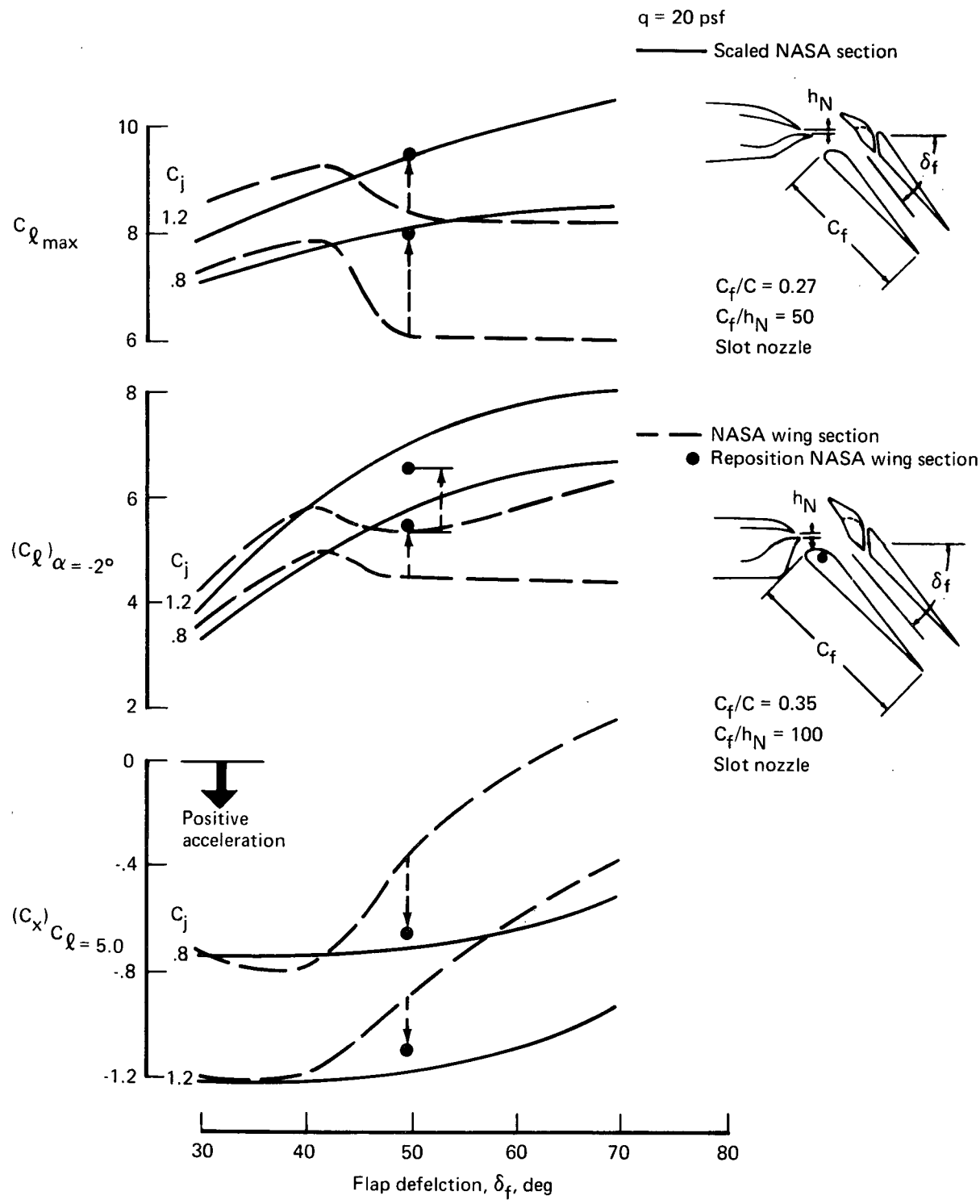

FIGURE 36.—COMPARISON OF FORCE DATA VARIATION WITH δ_f—NASA WING SECTION VERSUS SCALED NASA SECTION

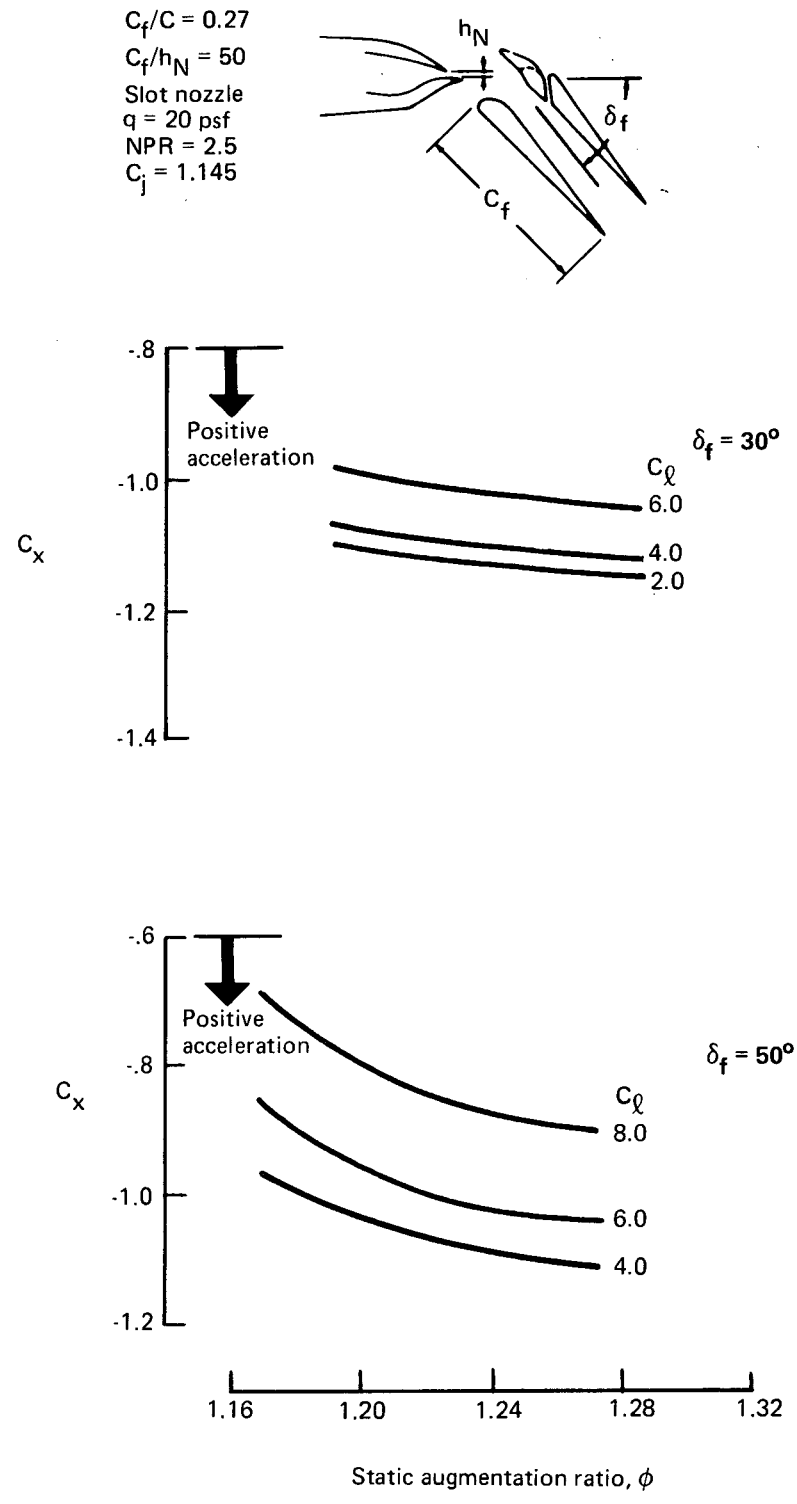

FIGURE 37.–EFFECT OF STATIC THRUST AUGMENTATION ON STREAMWISE FORCE AT FORWARD SPEED

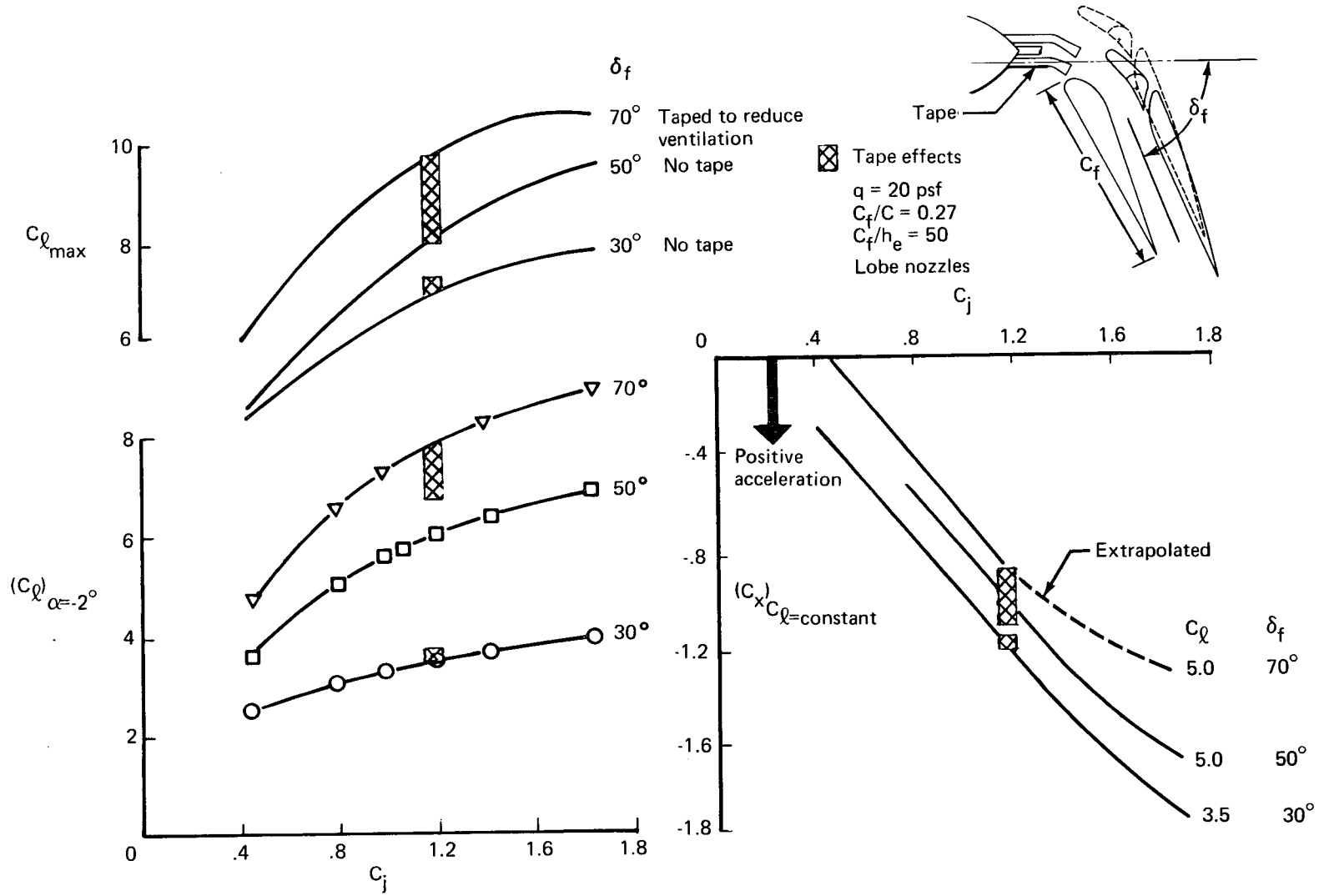

FIGURE 38.—VARIATION OF LIFT AND STREAMWISE FORCE WITH C_j FOR THE LOBE NOZZLE AUGMENTOR FLAP

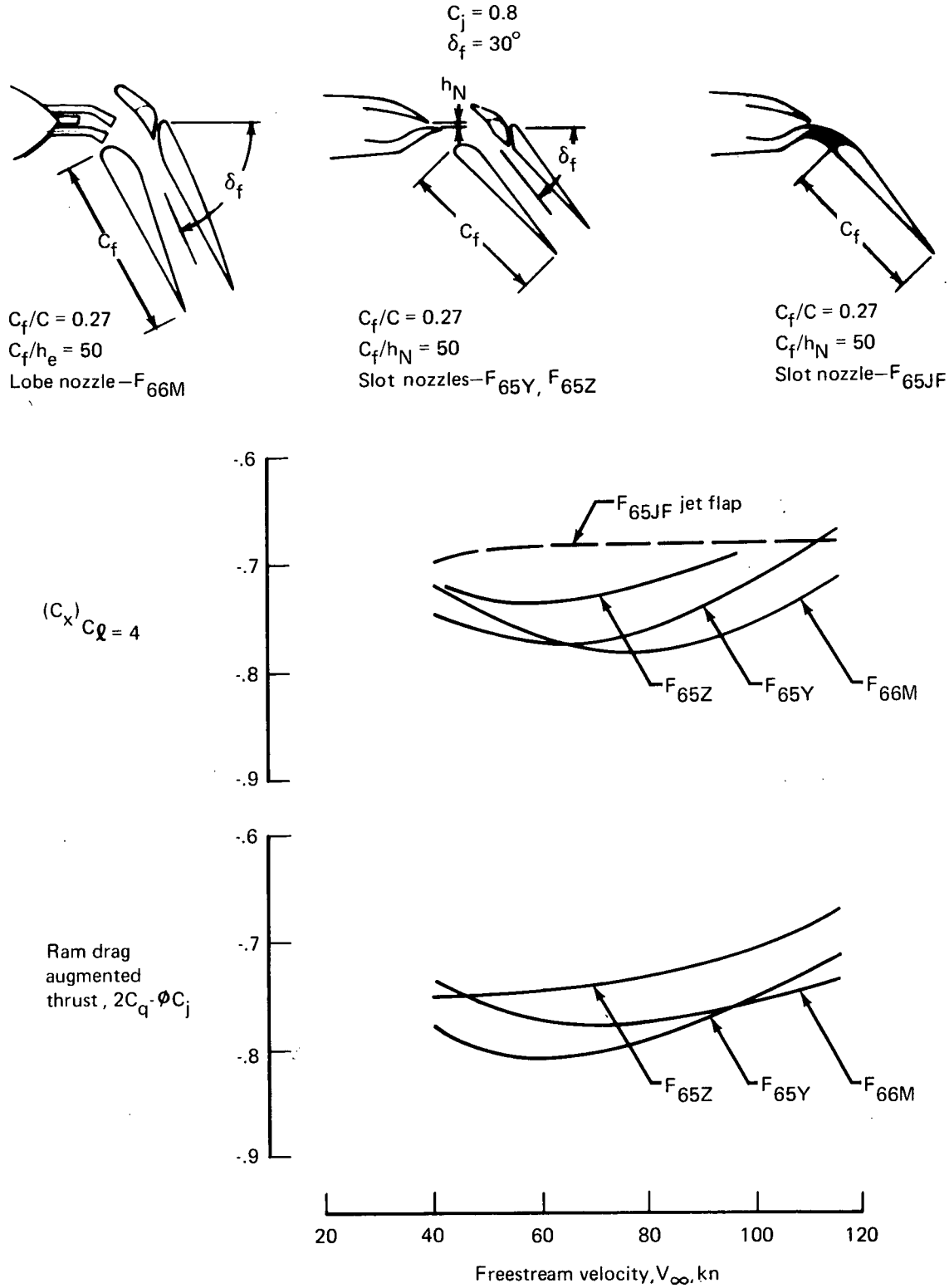

FIGURE 39.–EFFECT OF FORWARD SPEED AT CONSTANT C_j